In presenting the dissertation as a partial fulfillment of the requirements for an advanced degree from the Georgia Institute of Technology, I agree that the Library of the Institution shall make it available for inspection and circulation in accordance with its regulations governing materials of this type. I agree that permission to copy from, or to publish from, this dissertation may be granted by the professor under whose direction it was written, or, in his absence, by the dean of the Graduate Division when such copying or publication is solely for scholarly purposes and does not involve potential financial gain. It is understood that any copying from, or publication of, this dissertation which involves potential financial gain will not be allowed without written permission.

_____

_____

PHOTOPHORETIC FORCE ON SELECTED SUBSTANCES

A THESIS

Presented to

The Faculty of the Graduate Division

by

Mark Herbert Rosen

In Partial Fulfillment

of the Requirements for the Degree

Master of Science in Chemical Engineering

Georgia Institute of Technology

January, 1963

PHOTOPHORETIC FORCE ON SELECTED SUBSTANCES

Approved:

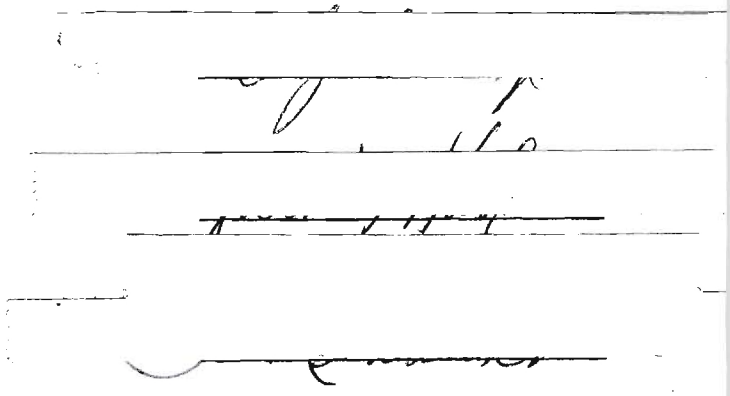

Date Approved by Chairman: Feb. 7, 1963

ACKNOWLEDGMENTS

The author wishes to acknowledge his indebtedness to his thesis advisor, Dr. Clyde Orr Jr., for his suggestions and constructive criticism of this work. He is also grateful to Mr. Warren Hendrix and Dr. F. K. Hurd for their help in the early stages of this work, and to Drs. R. F. Hochman and F. K. Hurd for their reading and evaluation of the text.

The assistance of the National Science Foundation is also gratefully acknowledged for the research grant making this work possible.

TABLE OF CONTENTS

TABLE OF CONTENTS (Continued)

LIST OF TABLES

LIST OF ILLUSTRATIONS

LIST OF ILLUSTRATIONS (Continued)

SUMMARY

Small gas-suspended particles encountering a light beam may be deflected either toward or away from the light source because of their uneven heating and their unequal interaction with the gas molecules. The phenomenon is called photophoresis.

This investigation of the photophoretic force was first undertaken by partially evacuating (1-20 mm. Hg) a glass bulb containing a small amount of finely divided material. The bulb was then agitated and the resulting aerosol, or gas suspension of particles, was exposed to the beam of a 150-watt projection lamp. By directing the light beam vertically upward, it was demonstrated that several powders (e.g., iron, zinc, gas carbon) could be suspended in a stationary position, or even moved upward against the gravitational force.

On the basis of these observations, a refined apparatus was constructed to enable measurement of particle velocities upward in the light beam and gravitational settling velocities downward in the absence of the beam. Settling velocity measurements establish the particle size and, with the upward movement data, permit a calculation to be made of the photophoretic force.

Although there were limitations on particle sizes, pressure range, and substances for which precise data could be obtained, the apparatus was successful in giving results within acceptable experimental error. The substances thoroughly investigated were gas carbon and wood charcoal. Measurements were made at pressures from 4.5 to 46 mm. of Hg. The majority

of the particles observed had radii between 5 and 25 microns and all were agglomerated. The use of agglomerated materials was found to be necessary because denser and better heat-conducting particles could not be suspended in the light beam of the intensity attained in the refined apparatus.

A dependence of photophoretic force on carrier gas pressure was detected and was found to agree in form with theoretical equations based on the radiometer interpretations of photophoresis. The dependence of photophoretic force on particle size and light intensity was determined and found also to compare well with the results predicted by theory.

The overall agreement between experimental results and those predicted by theory is good and gives strong support for the radiometer interpretation of photophoresis.

CHAPTER I

INTRODUCTION

Photophoresis may be defined as the migration of gas-suspended particles under the influence of an intense beam of light. This phenomenon has been the subject of considerable investigation since its observation was first reported by Enrenhaft (1). The direction and magnitude of the photophoretic force is a function of particle size, particle shape, gas pressure, light intensity, thermal conductivity, and possibly other factors.

The purpose of this investigation was to develop a new method of measuring photophoretic force, and to attempt to arrive at some relationships between photophoretic force and the above-mentioned variables. When better understood, photophoresis may have applications in particle classification, mineral beneficiation, gas cleaning, and the like.

Particle sizes were estimated from settling rate data, and photophoretic motion was measured in order to compute the force. Previous measurements have been made using techniques developed by Ehrenhaft (2) in which particle size was measured in a modified Millikan apparatus. This method involves manipulation of a charged particle in an electrostatic field. The particle is then exposed to two-sided illumination and particle velocities are measured. This two-sided illumination consists of horizontal opposing beams which are adjusted so that their contours coincide. The technique used for this investigation involved a single light beam direct vertically upward.

Many observers have carried out qualitative experiments concerning photophoresis with varying particle sizes, shapes, and materials. Of additional interest has been the effects of superimposed electrostatic and magnetic fields. A good discussion of photophoresis under these varying conditions is found in work done by Preining (3). The theoretical equations developed by Hettner (4) and Rubinowitz (5) are the most current, and Rohatschek (6) has written a good discussion on the qualitative and semi-quantitative theories of photophoresis. Mattauch (7) has perhaps done the most significant quantitative measurements in his work detecting the pressure dependence of photophoretic force.

CHAPTER II

APPARATUS

A. General

A photograph of the apparatus is shown in Figure 1. Its basic components are (1) a chamber in which air-suspended particles were exposed to the beam from an arc lamp (2) a solenoid-operated beam interrupter activated and timed by a thyratron device and (3) a slide wire variable resistor adapted to record the vertical displacement of the particles. Figure 2 identifies the various components pictured in Figure 1. Each component is described in detail below.

B. Aerosol Chamber

This chamber was approximately one foot long and three inches square, with a 1/8-inch wall thickness. At the top and bottom of the chamber were removable steel plates, the bottom plate having a 1/2-inch diameter hole that was covered by a quartz window to allow entrance of a light beam. The bottom plate was also fitted with three brass pins which, positioned tightly into countersunk holes in the plate on which the chamber rested in operation, ensured replacement of the chamber in the same position relative to the light beam each time it was removed. The chamber also had an 8 3/4-by 1/4-inch observation slit along one side covered by a Plexiglas window, and it was fitted with inlet and outlet lines opened and closed by manually operated valves. The inside of the chamber was

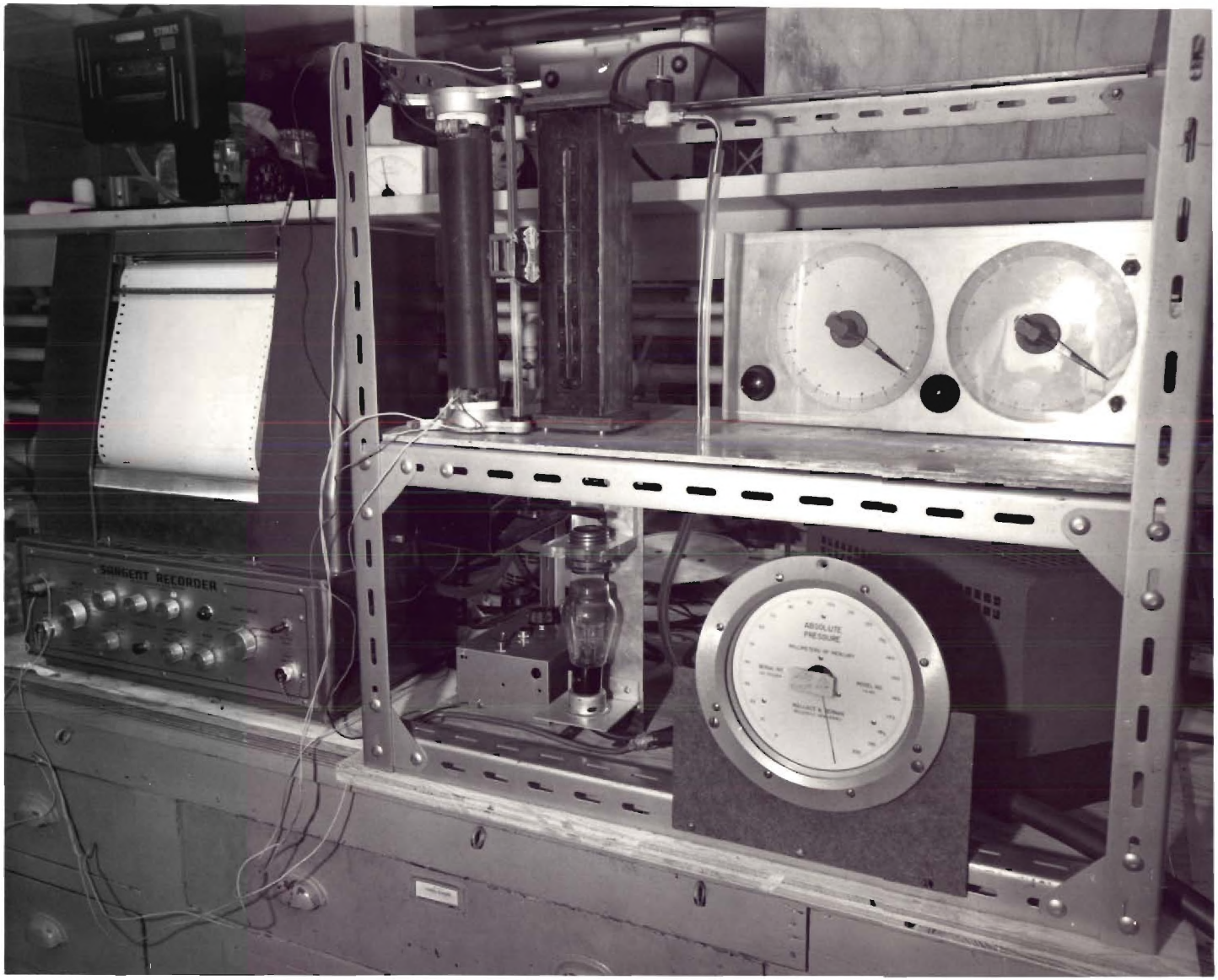

Figure 1. Apparatus for Determination of Photophoretic Force.

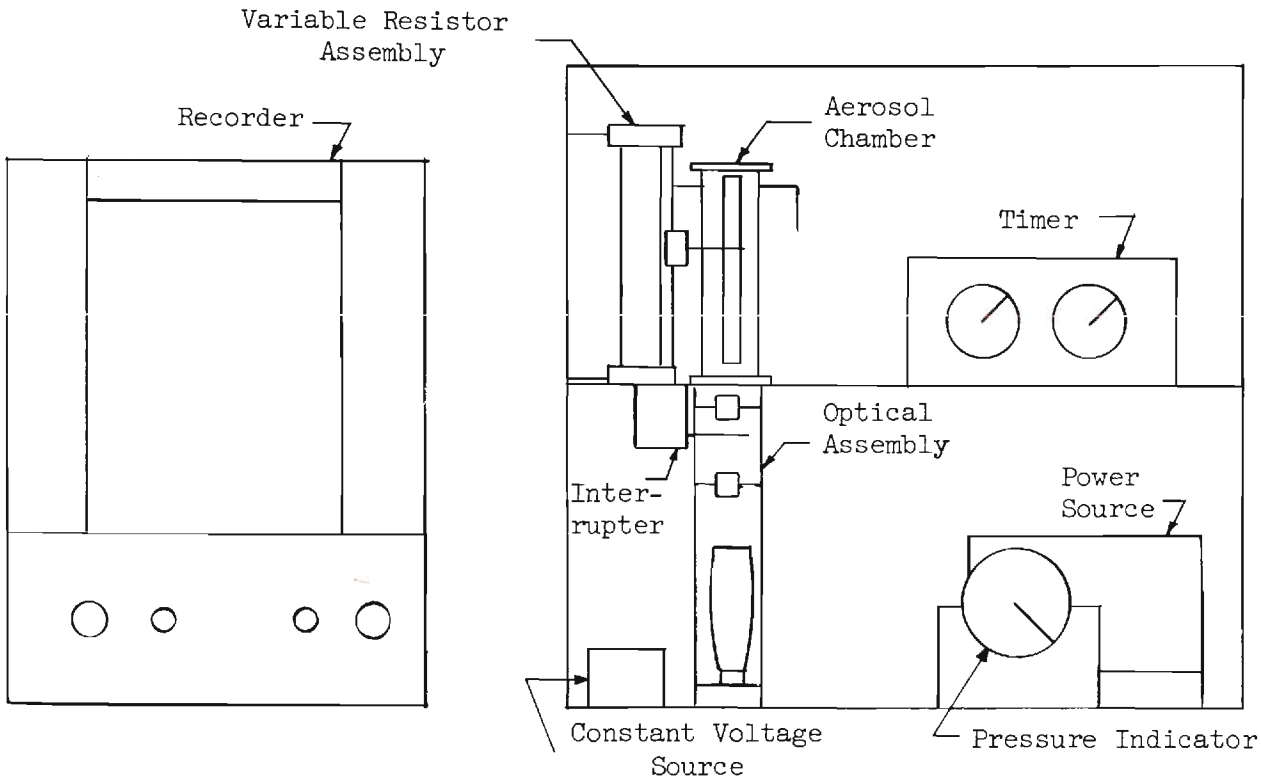

Figure 2. Block Diagram of Apparatus for Determination of Photophoretic Force.

painted with camera black to minimize scattered light. Figure 3 is a detailed drawing of the aerosol chamber.

C. Optics

The light source was a 100-watt, zirconium arc lamp, manufactured by Sylvania Electric Products, Inc., New York, N. Y. The lamp required 15.4 volts d.c. at 6.25 amperes and a momentary starting potential of 2000 volts obtained from a power supply, model G-157, of the Gaertner Scientific Corporation, Chicago, Ill. In order to produce a beam of light intense enough to produce photophoresis, an auxiliary optical system was required. Several lens combinations were tested, with the final system being built around two matched achromatic lenses, each having a 1 1/2-inch diameter and a 3/4-inch focal length. The first served as a condensing lens, and the second produced as nearly as possible a parallel beam of light approximately 1 1/2 cm in diameter. The lenses were mounted in threaded steel casings which were, in turn, mounted in a Plexiglas frame provided with a screw-type find adjustment. The Plexiglas frame was also movable for coarse adjustment. This assembly is shown in Figure 4. For measurement of the absolute intensity of the beam an Eppley Laboratories Inc., Newport, R. I., twelve-junction, iron-constantan thermopile was used in conjunction with a Model 8686 potentiometer of the Leeds and Northrup Co., Philadelphia, Pa.

D. Interrupter and Timer

Interruption of the light beam to obtain up-and-down particle movement was accomplished with two solenoids and a metal blade assembled such that activation of one solenoid caused the beam to be obstructed

Scale 1:3

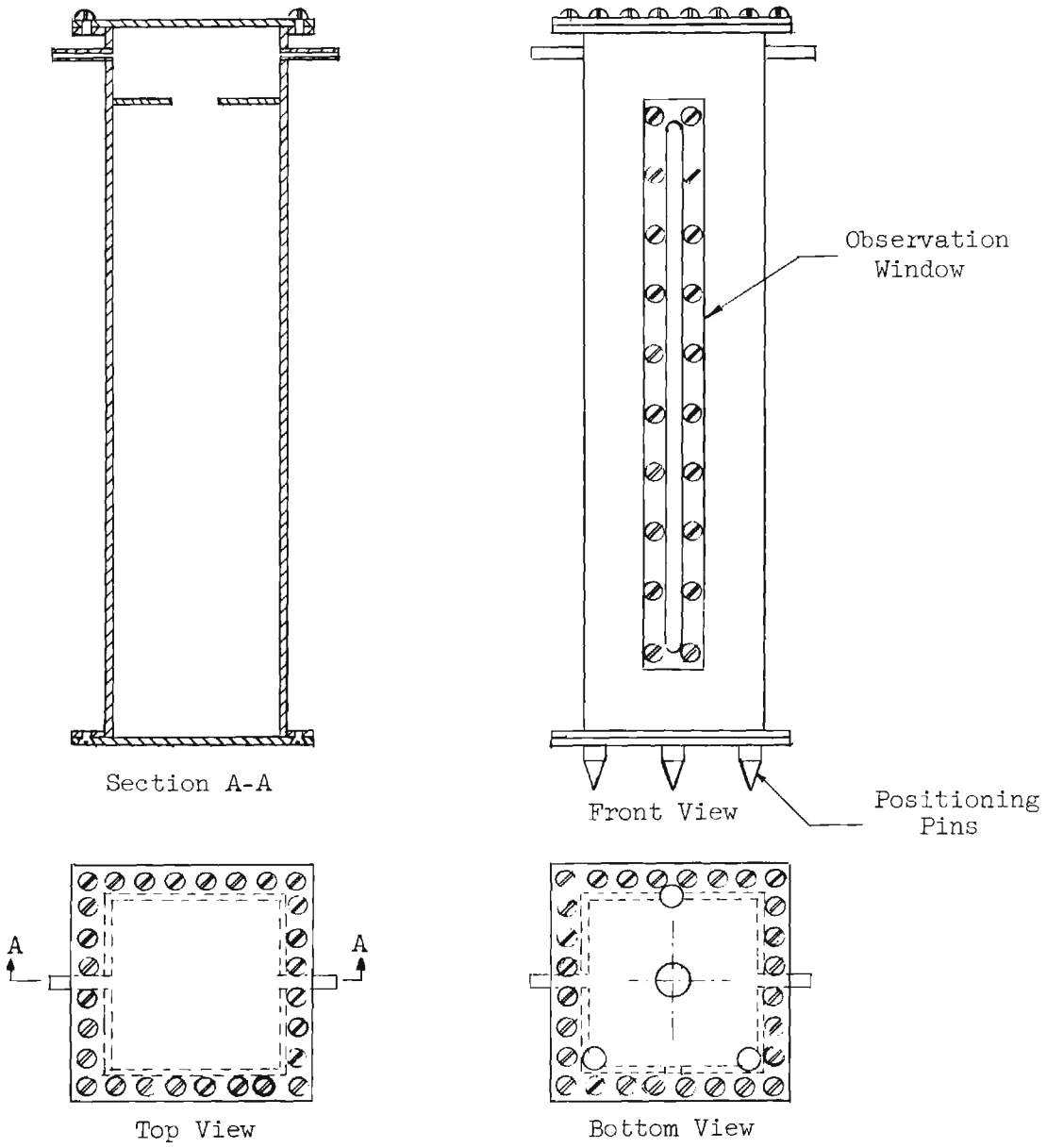

Figure 3. Aerosol Chamber Detail.

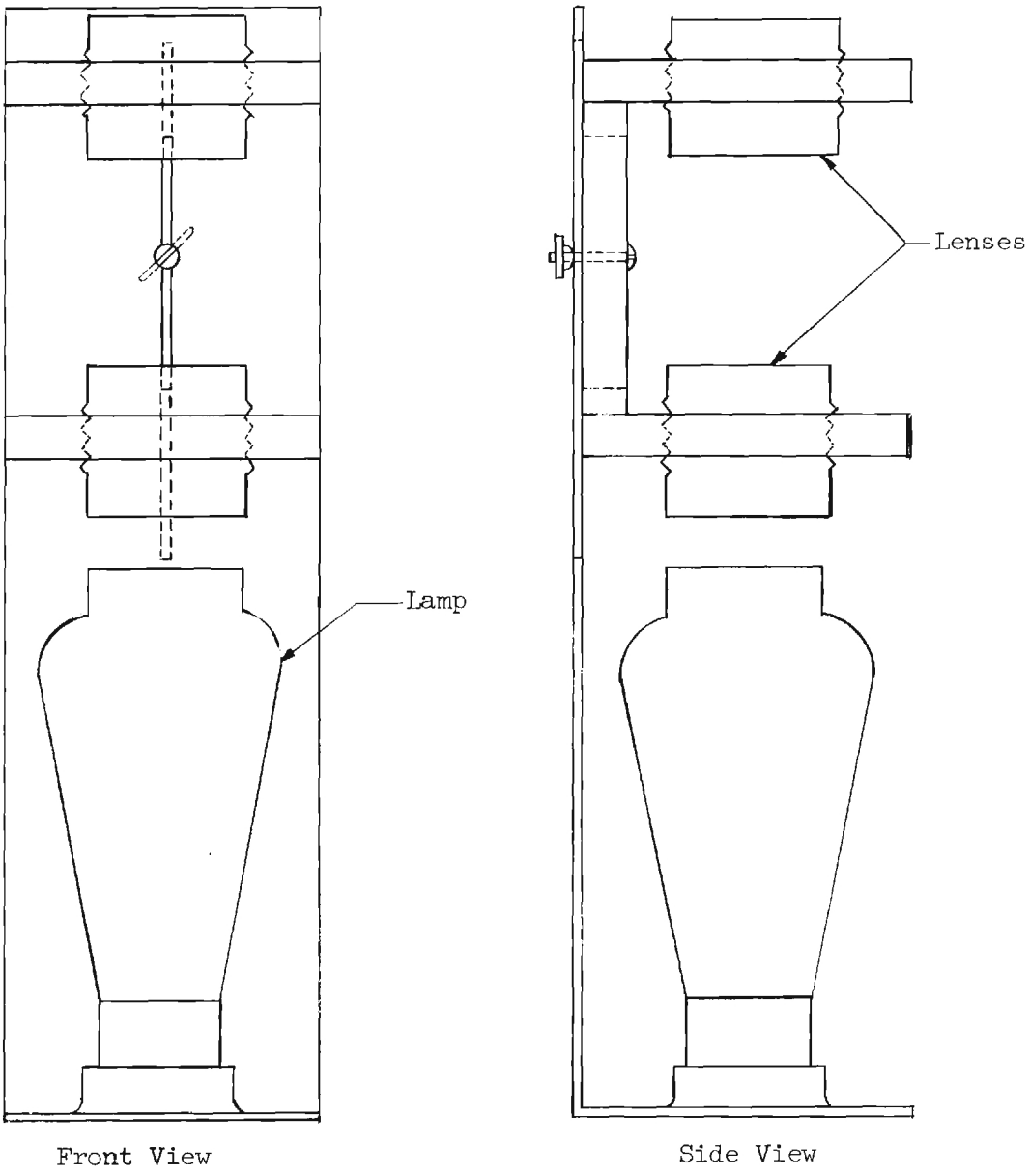

Figure 4. Optical Assembly.

from entering the aerosol chamber. Activation of the second solenoid then removed the blade from the beam. In order to time these intervals accurately, an adaption of a thyratron device described by Swenne (8) was constructed. Two such devices were coupled together, each operating one of the solenoids, such that activation of one and deactivation of the other occurred simultaneously. Activation times were established by rheostats in the timer. Thus the interrupter could be operated continuously at constant time intervals, with an accuracy of ±0.05 sec., without the necessity of individually timing each cycle. A circuit diagram of the timer is given as Figure 5.

E. Vertical Displacement

To measure the distance of rise and fall of the particles, a slide-wire resistor was fitted with a pointer and mounted so that a particle moving in the chamber could be followed with the pointer. By impressing a constant voltage across the resistor, changes in particle height in the chamber were translated into changes in emf, the latter being recorded on a Model S-72150 recorder of E. I. Sargent & Co., Chicago, Illinois. In this manner, distances of rise and fall were measured merely by following the particle with the pointer even though actual distances were not determined until after completion of an experiment. Figure 6 shows a circuit diagram of the voltage source and the variable resistor assembly.

F. Operation

The apparatus was designed so that one person might operate it without difficulty. An experiment was initiated by agitating the powder in the chamber and then singling out a particle caught in the light beam

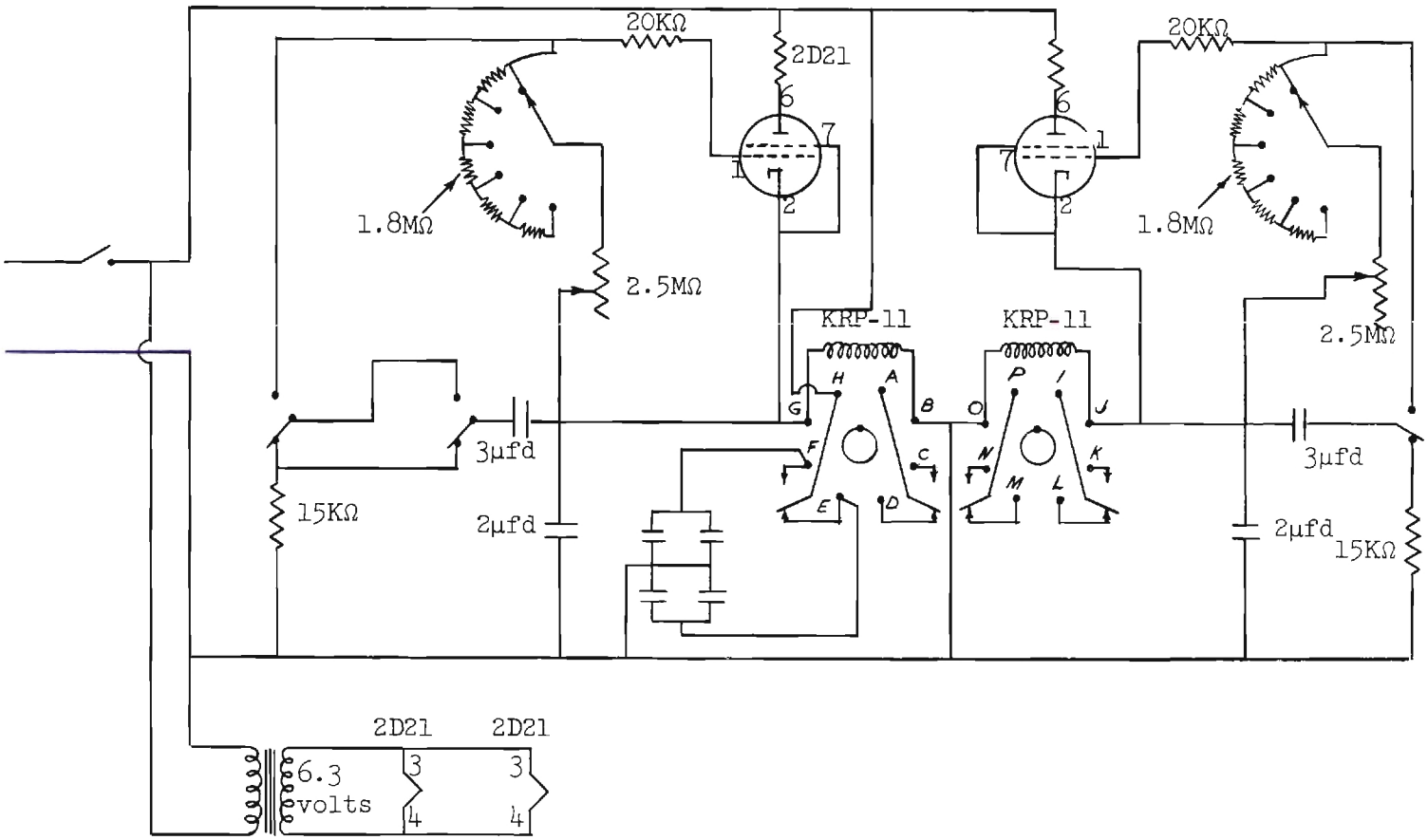

Figure 5. Circuit Diagram of Timer.

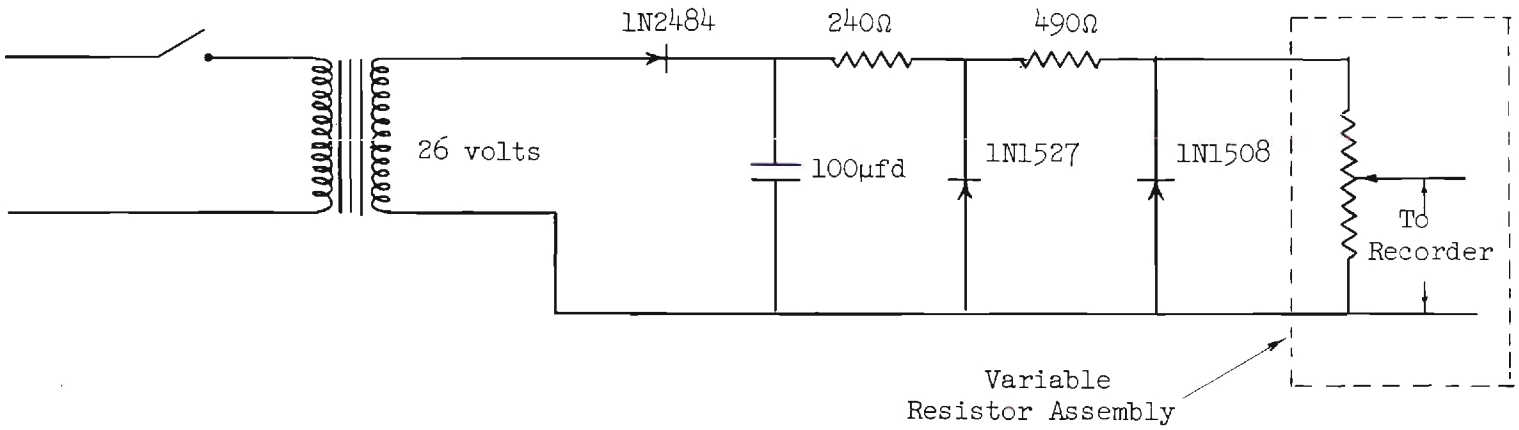

Figure 6. Circuit Diagram for Constant Voltage Source and Variable Resistor Assembly.

for study. The beam interrupter was started, and the time was adjusted so that the particle rose and fell in approximately the same position in the chamber. The particle, then, was followed with the pointer until sufficient data were obtained.

CHAPTER III

CALCULATION OF EXPERIMENTAL PHOTOPHORETIC FORCE

A. Evaluation of Particle Radius and Photophoretic Force

Once the rising and settling velocities of a particle have been experimentally determined, the photophoretic force may be calculated in the following manner:

A particle moving in a viscous medium under the influence of a constant force reaches a constant linear velocity V, that is determined by the force. This relationship may be expressed by

$$V = FZ \tag{1}$$

where Z, the mobility (9) of the particle, is characteristic of particle size and shape and of the properties of the fluid medium. For a sphere in a homogeneous medium, the mobility is given by

$$Z = \frac{1}{6\pi\mu a} \tag{2}$$

a form of Stokes law where μ is the medium viscosity and a the particle radius. As the mean free path becomes comparable to the particle size, equation 2 must be modified by inclusion of a slip correction factor S. The mobility is then defined by

$$Z = \frac{S}{6\pi\mu a} \tag{3}$$

The slip correction is a function of $\frac{\lambda}{a}$, where λ is the mean free path of the gas molecules and a, as before, is the particle radius. The correction accounts for the tendency of a particle to slip between molecules of the fluid (10,11,12).

When the velocity in equation 1 is the settling velocity V_s, then F becomes the gravitational force acting on the particle, defined by

$$F_g = \frac{4}{3} \pi a^3 g_c \rho_p \tag{4}$$

where g_c is the gravitational constant and ρ_p is the particle density. Substituting equation 1 into equation 4 and solving for a gives

$$a = \left(\frac{9 V_s \mu}{2S g_c \rho_p} \right)^{1/2} \tag{5}$$

Having determined the particle radius, the photophoretic force, F_p, is then evaluated by

$$F_p = F_d + F_g \tag{6}$$

where F_d is the drag force exerted by the fluid on the rising particle. Substituting equations 1 and 4 into equation 6 gives

$$F_p = \frac{V_r}{SZ} + \frac{4}{3} \pi a^3 g_c \rho_p \tag{7}$$

where V_r is the velocity of the rising particle.

B. Mean Free Path of Air Molecules and Slip Factor Evaluation

In order to apply the equations developed above, the mean free path length of the carrier gas and the resulting slip factor must be evaluated. The mean free path, λ, is given by

$$\lambda = \frac{\mu R T}{0.499 M P \bar{V}} \tag{8}$$

where $\bar{V}$, the mean molecular speed, is defined by $\bar{V} = (8g_c RT/\pi M)^{1/2}$, where T is the absolute temperature, R is the universal gas constant, and M is the molecular weight of the gas.

The slip effect as mentioned in the preceding section was defined by Knudsen and Weber (13) by the empirical relationship

$$S = 1 + \frac{\lambda}{a}\left(A + Be^{-C\frac{a}{\lambda}}\right) \tag{9}$$

The proper value of the empirical constants A, B, and C, according to an analysis by Davies (12) with air as the fluid medium, are A = 1.257, B = 0.400, and C = 1.10.

C. Computation

Solution of the equation resulting from the combinations of equations 5 and 9 was facilitated by use of the Burroughs 220 digital computer. A program was written enabling each series of particle radii and corresponding photophoretic forces to be evaluated for several values of apparent density. The need for this will be shown in section VI-E.

CHAPTER IV

CALCULATION OF THEORETICAL PHOTOPHORETIC FORCE

A suitable theory explaining the phenomenon of photophoresis is not wholly agreed upon, although most investigators believe it to be a radiometer effect (6,14,15,16,17). The strongest support for the radiometer theory lies in the relationship between the pressure of the surrounding gas and the photophoretic force acting on a particle. This force F_R has been shown to exhibit a maximum value at a pressure P_{max} such that the mean free path length is equal to the acting dimensions of the particle. Below this pressure the force is directly proportional to pressure, while above it an inverse proportionality exists. This characteristic of photophoresis is found in radiometer theory developed by Epstein (18), and later, Weber (19). Weber's equation, for a constant temperature difference, assumes the following form in reduced representation:

$$\frac{F_R}{(F_R)_{max}} = \frac{2 + \gamma}{\frac{P}{P_{max}} + \frac{P_{max}}{P} + \gamma} \qquad (10)$$

The value of the constant γ is determined by the geometry of the radiometer and an accommodation coefficient. While this expression is a useful tool in examining experimental data, it actually does no more than demonstrate a similarity between radiometer force and photophoretic force.

It is obvious from the above that two mechanisms exist for radiometer forces, one for high pressures and another for low pressures (high

and low pressures being defined as discussed above). Rubinowitz (5) has derived an expression based on molecular kinetic theory for the low pressure region, in which the radiometer force for spheres is equal to

$$F_R = \frac{\pi \alpha P a^3 G_p}{3T} \tag{11}$$

where α is the accommodation coefficient and G_p is the temperature gradient inside a particle.

Hettner (4) has developed an equation for the high pressure mechanism, describing the radiometer force for spheres by

$$F_R = - \frac{3\pi \mu^2 a R G_p}{P M} \tag{12}$$

Hettner has also submitted the following empirical interpolated equation for the transition region (λ comparable to $\underline{a}$):

$$F_R = \frac{\pi a^2 \mu (\alpha R/MT)^{1/2} G_p}{\frac{P}{P_{max}} + \frac{P_{max}}{P}} \tag{13}$$

where

$$P_{max} = \frac{3\mu}{a} (RT/M)^{1/2} \tag{14}$$

The major problem in attempting to apply these equations to photophoresis is in evaluation of the gradient G_p. Rubinowitz (5) has derived an expression for G_p at high pressures for spherical particles exposed to one sided illumination. His equation is

$$G_p = \frac{I}{2(X_p + X_M)} \tag{15}$$

where I is absolute luminous intensity, X_p is particle thermal conductivity, and X_M is the thermal conductivity of the surrounding medium. Thus the force in this case is

$$F_R = - \frac{3 \mu^2 a R I}{2P M (X_p + X_m)} \tag{16}$$

If a particle is non-transparent, but is not absolutely black, $I\sigma$ must be substituted for I, where σ is the coefficient of light absorption.

It must be remembered that these equations apply only if photophoresis is assumed to be a radiometer effect. Several investigators have challenged this concept (20, 21, 22), and it can by no means be accepted as fact.

Ehrenhaft (22) has enumerated several facts contradicting the radiometer interpretation of photophoresis. He contends that photophoresis is a first order electromagnetic effect.

CHAPTER V

RESULTS

A. Qualitative

Many variations of photophoretic movement were observed during the course of experimentation. The temperature distribution in a particle exposed to radiation is greatly affected by its shape and state of agglomeration. Wings and points will be cooler, and irregularly shaped particles travel in various unusual paths. Screw-type movement is common, as is closed orbiting in elliptical, circular, and circular-spiral paths. This stable orbiting may vary from orbits of very small diameter accompanied with high revolutions per second, to slower moving particles with large orbital paths. Many orbiting particles were suspended in an equilibrium position in the beam for several minutes and apparently would have remained indefinitely. In early observations with the projection lamp, in which the beam intensity was variable, an increase in orbital diameter along with a decrease in angular velocity was observed with decreasing intensity.

A detailed description of these movements and others is given by Preining (3), whose observations concur with those made in this study.

B. Quantitative

A great many particles of a variety of materials were observed in the apparatus, but wood charcoal and gas carbon were the only two that experienced sufficient photophoretic force to be measurable (see section VI-D). Electron micrographs showed both to be composed of agglomerates

of particles with the average primary particle diameter being approximately 0.25 micron for the charcoal and 0.05 micron for the gas carbon. The agglomerates were generally about 5 to 25 microns in diameter. The experimental procedure was to maintain a constant pressure in the chamber and obtain velocity data for from 10 to 15 particles at that pressure. Data were then taken for several pressures within the above-mentioned ranges. The measured photophoretic force was plotted versus particle radius for each pressure. A representative plot of this type is shown in Figure 7. The bulk of the data is tabulated and plotted in Appendix B.

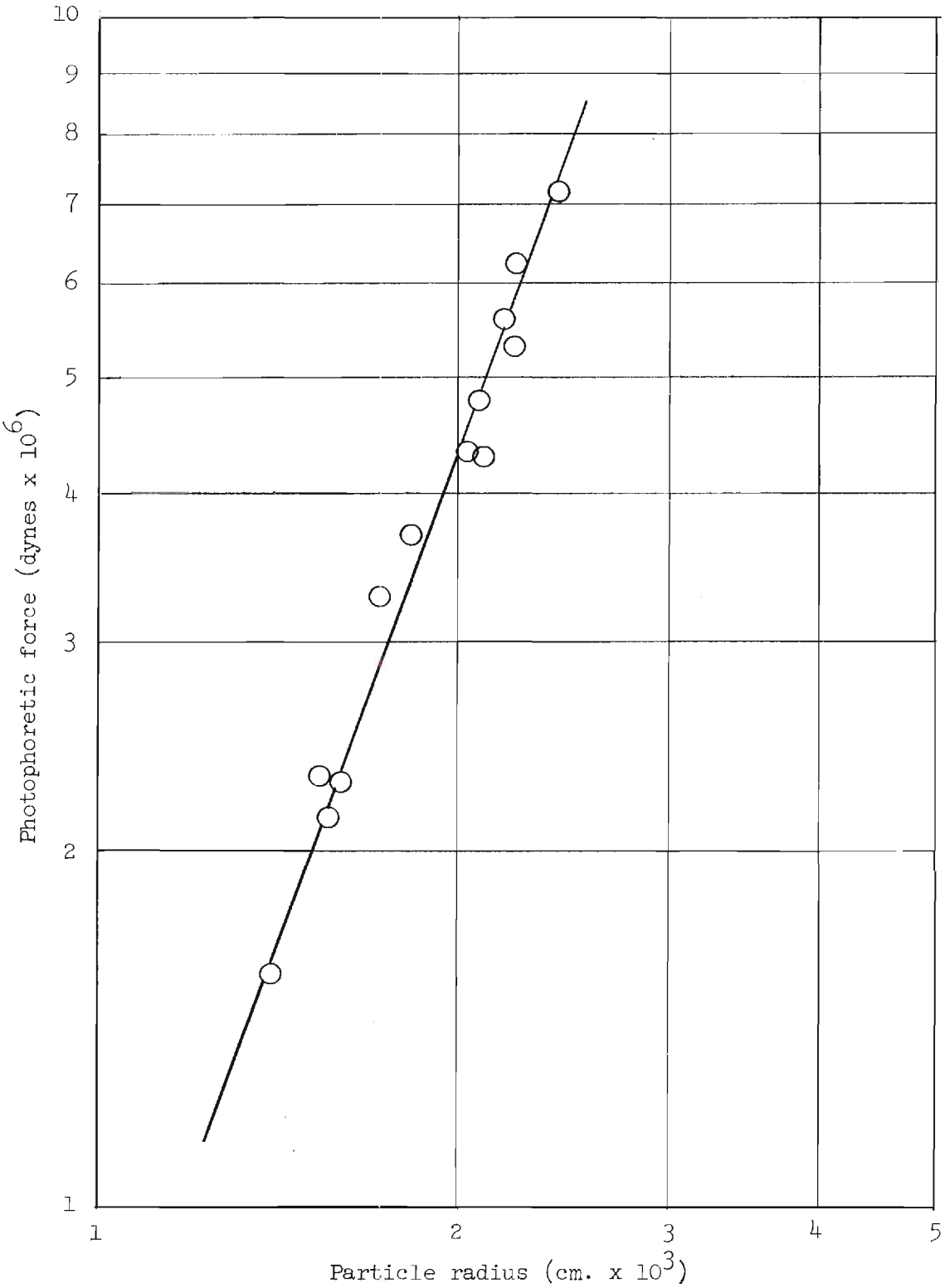

Figure 7. Photophoretic Force versus Particle Radius for Gas Carbon at 15.3 mm. Hg.

CHAPTER VI

DISCUSSION OF RESULTS

A. Dependence of Photophoretic Force on Particle Radius

Equations 11, 12, and 13 require that photophoretic force be proportional to the cube of the radius at low pressure, to the square of the radius at intermediate pressures, and linearly proportional at high pressures. The value of the exponent of the radius is determined by the slopes of the log-log plots presented in figures 7 and 14 through 21 (given in the Appendix). Table 1 gives the values of these slopes.

Table 1. Exponent on Radius Term for Carbon Particles as a Function of Gas Pressure

Pressure (mm. Hg)	Exponent
8.3	2.72
15.3	2.78
25.6	2.30
35.4	1.86
46	1.8

For a 20 micron particle, 1 mm. of Hg is in approximately the middle of the intermediate pressure range. The values of the exponent follow the trend predicted by theory well, although they are somewhat larger than the equations predict.

B. Dependence of Photophoretic Force on Gas Pressure

Several previous investigators have been unable to detect a pressure dependence in photophoretic force. This was probably due to the fact that they were working in the pressure region of maximum force for the size particles they were observing (see equation 14). This condition occurs in much of the data gathered in this investigation; however, it was possible to detect a definite pressure dependence. Figure 8 shows pressure versus force for three particle radii. For the 15 micron particle, the force is very nearly constant for the entire pressure range, indicating that the force is in a region of maximum value. As the particle radius increases displacing the maximum force region to a lower pressure, the pressure dependence becomes noticeable. Table 2 shows pressure and force data for several radii for gas carbon and wood charcoal. It may be seen that for wood charcoal the 5 micron particle shows a maximum between 9.7 and 21.3 mm. Hg pressure. Figure 9 shows a rough plot of these data. According to equation 14, the maximum force should occur at about 25 mm. Hg, which is fair agreement between experimental results and theory. To test the general form of equation 13, one data point for a 25 micron gas carbon particle was assumed to lie on the theoretical curve. From this point, the numerator of the right side of equation 13 was calculated and subsequently used to complete the theoretical curve. Figure 10 shows the results of this computation. The two curves follow the same general pattern, although the experimental data appear to be approaching constancy more rapidly.

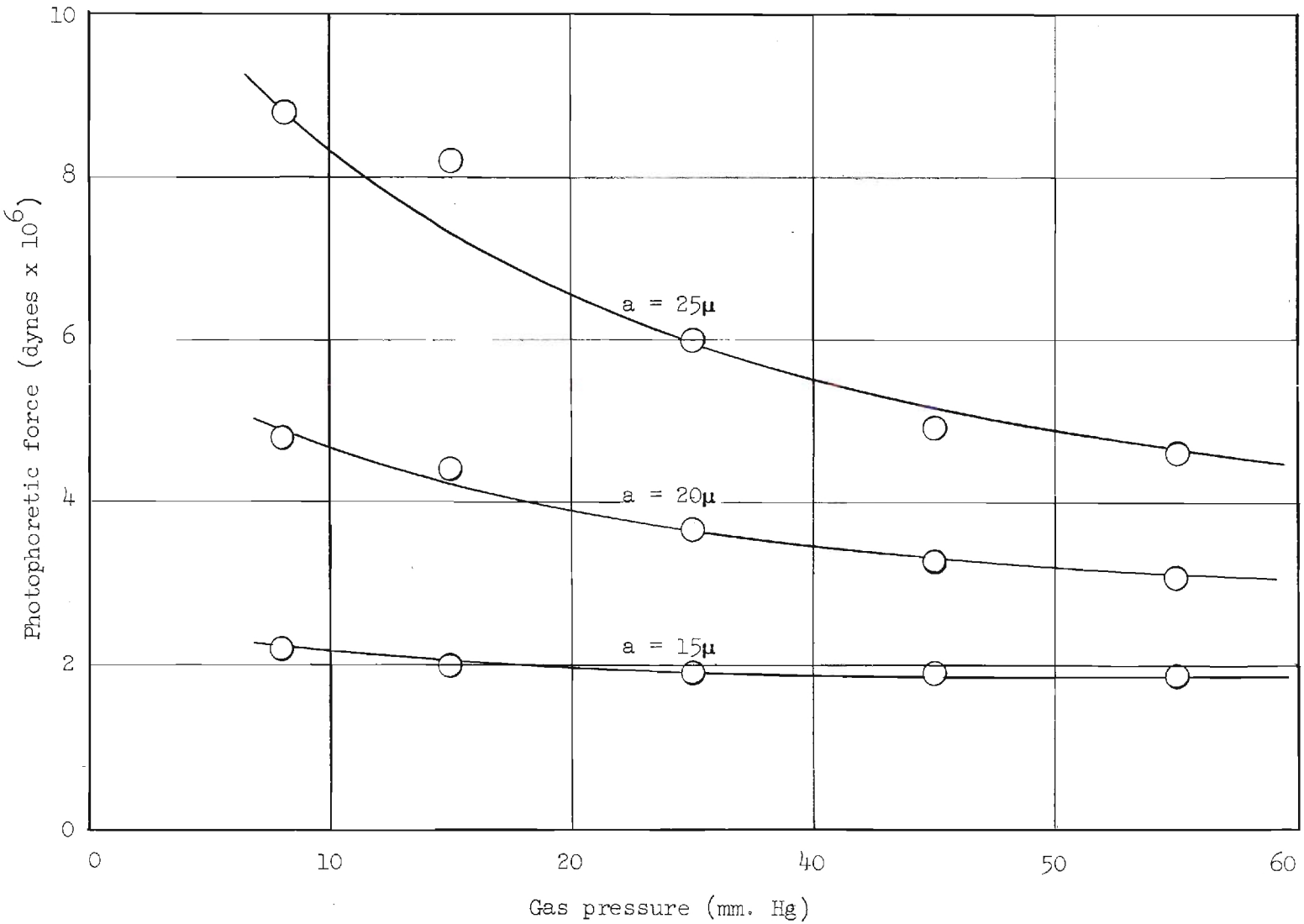

Figure 8. Photophoretic Force versus Gas Pressure for Gas Carbon Particles.

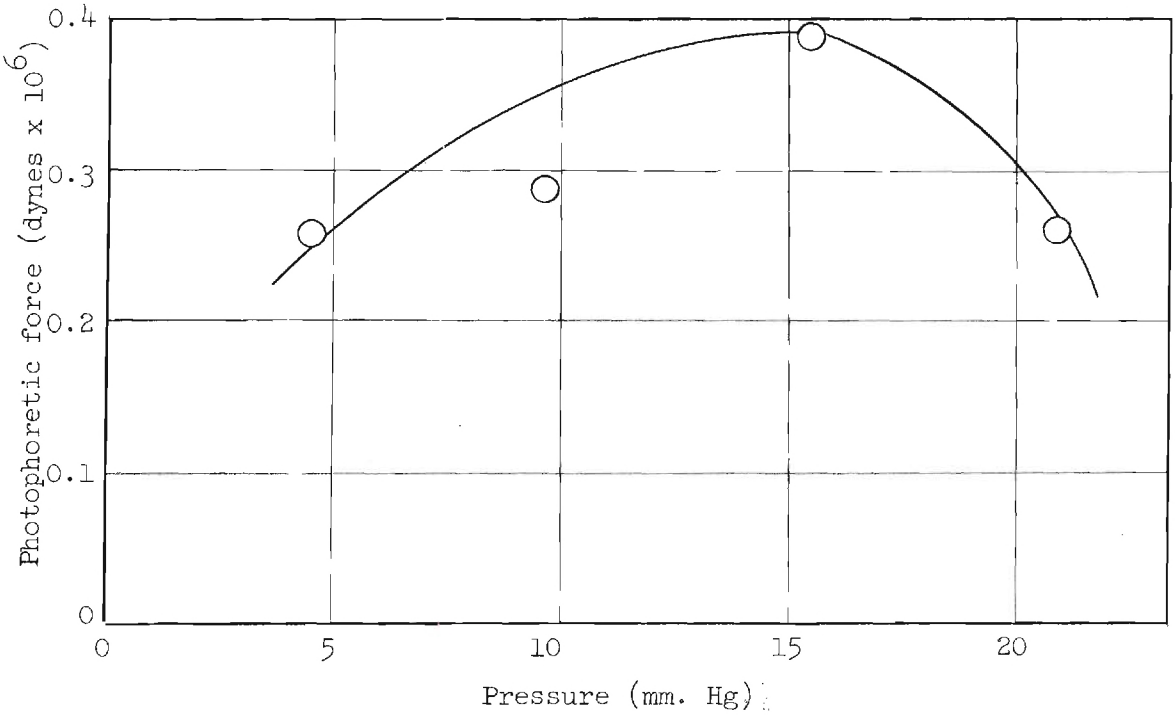

Figure 9. Photophoretic Force versus Pressure for Five Micron Radius Wood Charcoal Particles.

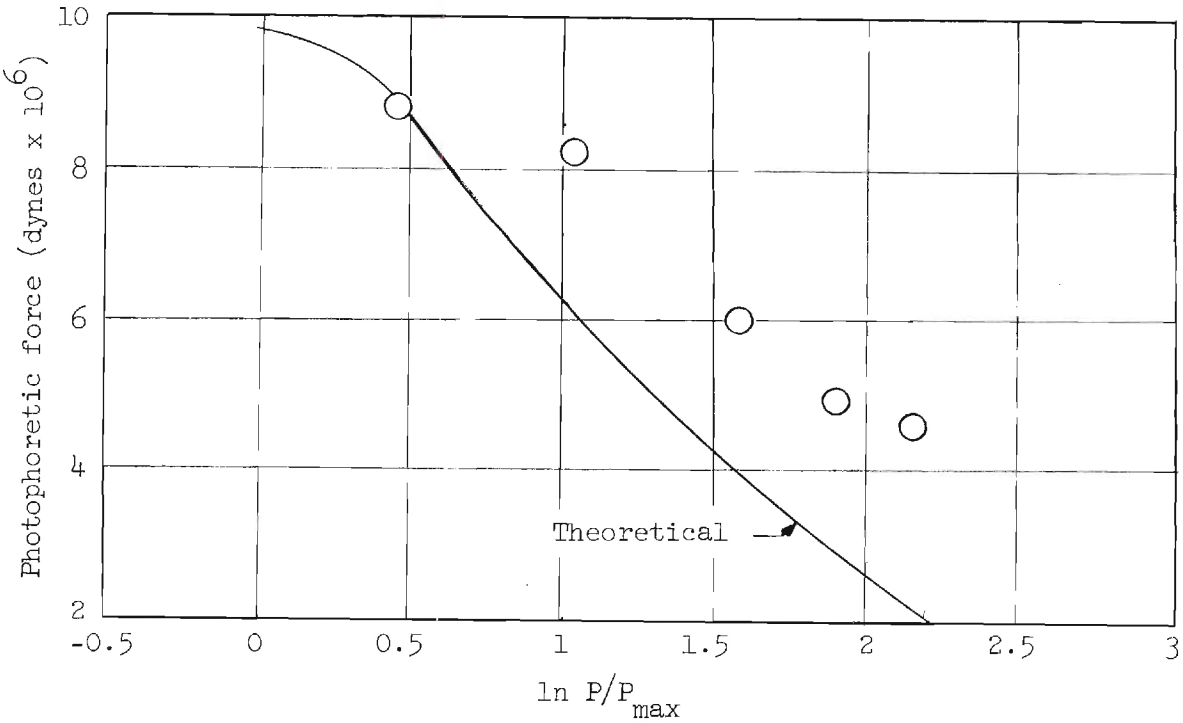

Figure 10. Comparison of Theoretical and Experimental Curves for 25 Micron Radius Gas Carbon Particles.

Table 2. Pressure and Force Data for Gas Carbon and Wood Charcoal Particles

Particle Radius (microns)	Pressure (mm. Hg)	Photophoretic Force (dynes x 10^6)
	Gas Carbon	
15	8.3	2.20
15	15.3	2.00
15	25.6	1.90
15	35.4	1.90
15	46.0	1.85
20	8.3	4.80
20	15.3	4.40
20	25.6	3.65
20	35.4	3.25
20	46.0	3.05
25	8.3	8.80
25	15.3	8.20
25	25.6	6.00
25	35.4	4.90
25	46.0	4.60
	Wood Charcoal	
5	4.7	2.60
5	9.7	2.75
5	15.6	3.90
5	21.3	2.60
10	4.7	2.05
10	9.7	2.00
10	15.6	2.10
10	21.3	2.10

C. Dependence of Photophoretic Force on Particle Thermal Conductivity

In agglomerated particles, the thermal conductivity may range between that of the solid to a value near that of the carrier gas (see section VI-E). In order to evaluate the applicability of equation 16, theoretical values were calculated for both extremes of thermal conductivity. Figure 11 shows the results of these computations. The upper and lower curves represent the values computed from equation 16, using the minimum and maximum conductivity values, respectively. The central curve is the experimental data. These curves indicate, as might be expected, that the particle conductivity is a function of the radius and approaches the conductivity of air with increasing size.

D. Dependence of Photophoretic Force on Light Intensity

According to radiometer thory, radiometer forces are directly proportional to light intensity. The intensity of the arc lamps used could not be varied; however, during the course of experimentation two different lamps were used, the ratio of their intensities being about 1.35. A comparison of the experimental forces results in a ratio of force of 1.30 - 1.40, indication that the intensity-force relationship is in fact one of direct proportionality. Figure 12 shows representative sets of data at 25 mm. Hg pressure for each lamp.

E. Determination of Effective Density and Thermal Conductivity

One of the most serious problems encountered in this investigation was the determination of effective particle densities. Fuks (23) cites cases where effective densities of agglomerated particles can be as low as 0.005 of the theoretical value. Work has been done in the Micromeri-

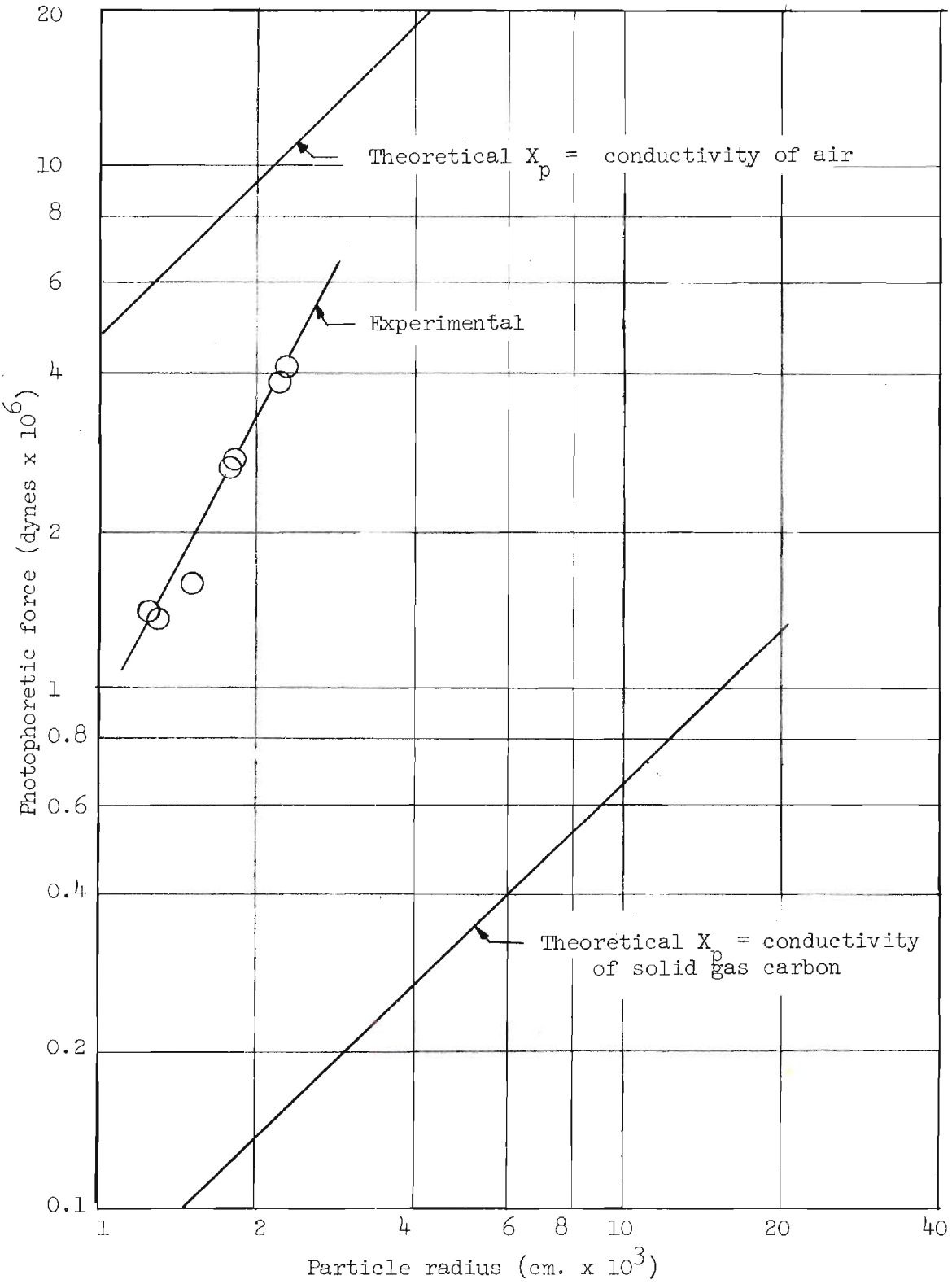

Figure 11. Comparison of Theoretical and Experimental Curves for Gas Carbon Particles at 35.4 mm. Hg.

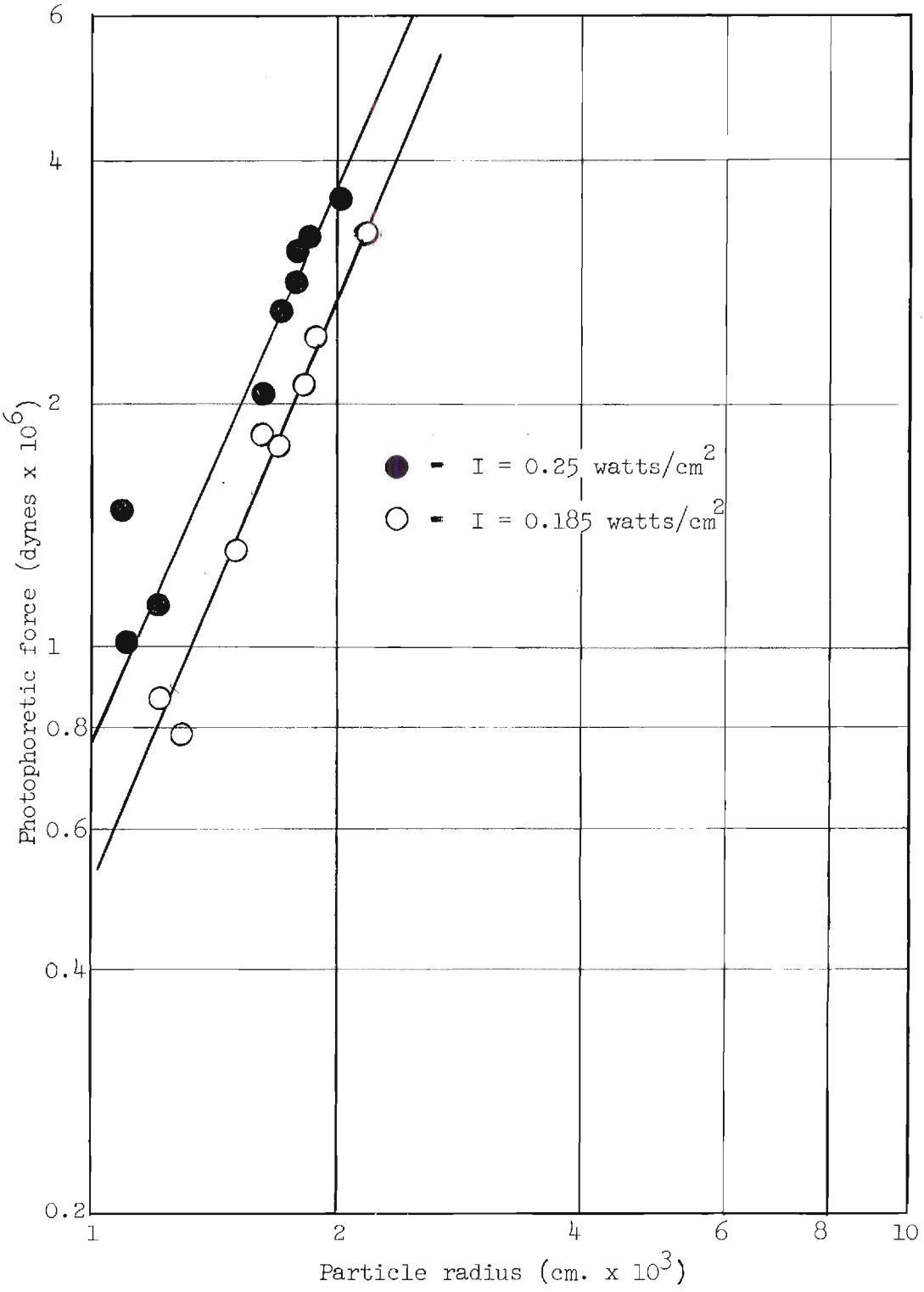

Figure 12. Comparison of Data for Gas Carbon Particles at 25 mm. Hg Taken at Different Light Intensities.

tics Laboratory of the Georgia Institute of Technology concerning the density of the wood charcoal used for this investigation. Since the density varies with agglomerate size, four different experimental methods were used to cover the entire size range from the bulk density to near the absolute density of the individual crystals. Bulk density was determined by weighing volumes of charcoal, and maximum density was obtained by use of pynconometers with carbon tetrachloride as the wetting agent. Intermediate values were obtained from settling rate data using an elutriator for larger sizes and a Millikan-type apparatus in conjunction with a cloud generator (developed by the Xerox Corporation, Rochester, N. Y.) for smaller sizes. The density versus size curve resulting from this investigation is shown in Appendix A. Using the digital computer, particle sizes and photophoretic forces were determined for 9 values of density between the bulk value (0.39 gms/cm) and the maximum value (1.37 gms/cm^3). The computed sizes were then matched to the experimental density-size curve so that the density used in calculating the size and the actual density were the same.

The average primary crystal size of the gas carbon was considerably smaller than that of the wood charcoal (0.05 micron as compared to 1.25 microns). Therefore, it was assumed that if a density-size curve had been determined for gas carbon, the particles observed would have fallen on the flat portion of the curve, and the bulk density value could be used. This value was measured and found to be 0.079 gms/cm^3.

As discussed in section VI-C, the thermal conductivity of agglomerated particles may vary over a wide range of values. Investigations of thermal conductivity of powders have been made (24,25,26) and simple

correlations based on porosity and solid and gas conductivity have been developed. However, these correlations become increasingly unreliable as the void fraction becomes larger, as is the case for very fine particles. Based on the above mentioned investigations, the conductivity of the wood charcoal and gas carbon should be very near that of the carrier gas (air in this case). Exact determination of the thermal conductivity becomes almost an arbitrary choice due to the uncertainty of quantities such as porosity. Therefore, no actual values were chosen as correct. The experimental data instead were compared to theoretical values calculated for conductivity extremes (Figure 11).

F. Limitations

There are several limitations inherent in the apparatus and techniques used in this investigation. Perhaps the most serious is the fact that only certain materials of very low density exhibit sufficient photophoretic force for the force to be measured. A great many substances were tested, including several metals (i.e., zinc, aluminum, iron), organic dyes, metal oxides, and liquid aerosols, including cotton seed and linseed oils and solutions of various dyes in water. These substances did not experience sufficient photophoresis to overcome gravitational forces. The use of a more intense light source would probably rectify this condition.

The apparatus also imposed limitations as to particle size. Since observation is by the unaided eye, particles below about 5 microns were too small to see. This condition automatically imposed a pressure restriction on observations since at higher pressures the force becomes small for

larger particles. It should be noted, however, that previous investigators have been limited to sub-micron particles, since larger particles exhibit velocities too great for the Millikan type apparatus.

G. Error Analysis

The most significant error sources are those involved in the estimation of particle properties, particularly the effective density. Although the densities used are believed to be good approximations of the true values, errors of as much as 200 to 300 per cent are not inconceivable. In addition, the equations used are based on the assumption that the particles are spherical. This is not strictly true, although it appears that most of the particles approximate spherical configuration.

Experimental errors are less significant than those mentioned above. Only data in which particle velocities for a single particle deviated by no more than 10 to 15 per cent were used. In many cases, the deviation was less than this.

Overall, the consistency of experimental data and agreement with theory must be considered good. Most of the points of Figures 7 and 14 through 21 deviate from the curve by no more than 15 per cent, and while the comparisons with theory shown in Figures 10 and 11 show greater error, they are considered within the limits to be expected.

CHAPTER VII

CONCLUSIONS

From this study, it is concluded that:

1. Measurement of rising and settling velocities in a vertical light beam provides an accurate method for determining photophoretic force.

2. The results show a definite pressure dependence to be present in photophoretic force and to follow closely that predicted from radiometer theory.

3. Relationships between particle size and light intensity also agree well with radiometer theory.

4. The overall results of this study give strong support to interpretation of photophoresis as a radiometer effect.

CHAPTER VIII

RECOMMENDATIONS

It is recommended that additional work be done with the same type of apparatus as used in this investigation but with consideration given to the following improvements. A more intense light source should be used, so that data may be obtained for more substances, particularly particles known to be single crystals for which densities and thermal conductivities are more accurately known. The possibility of an additional optical system for observing and following the particles should be investigated in order to increase the particle size and pressure ranges over which data can be taken. In addition to more exacting data on the relationship of photophoreses to the variables discussed in this report, work should be done to determine the dependence of photophoretic force on variables such as the wave length of the light and the nature of the carrier gas. This would permit a better understanding of photophoresis to be attained.

APPENDIX A

EFFECTIVE DENSITY - PARTICLE SIZE CURVE FOR WOOD CHARCOAL

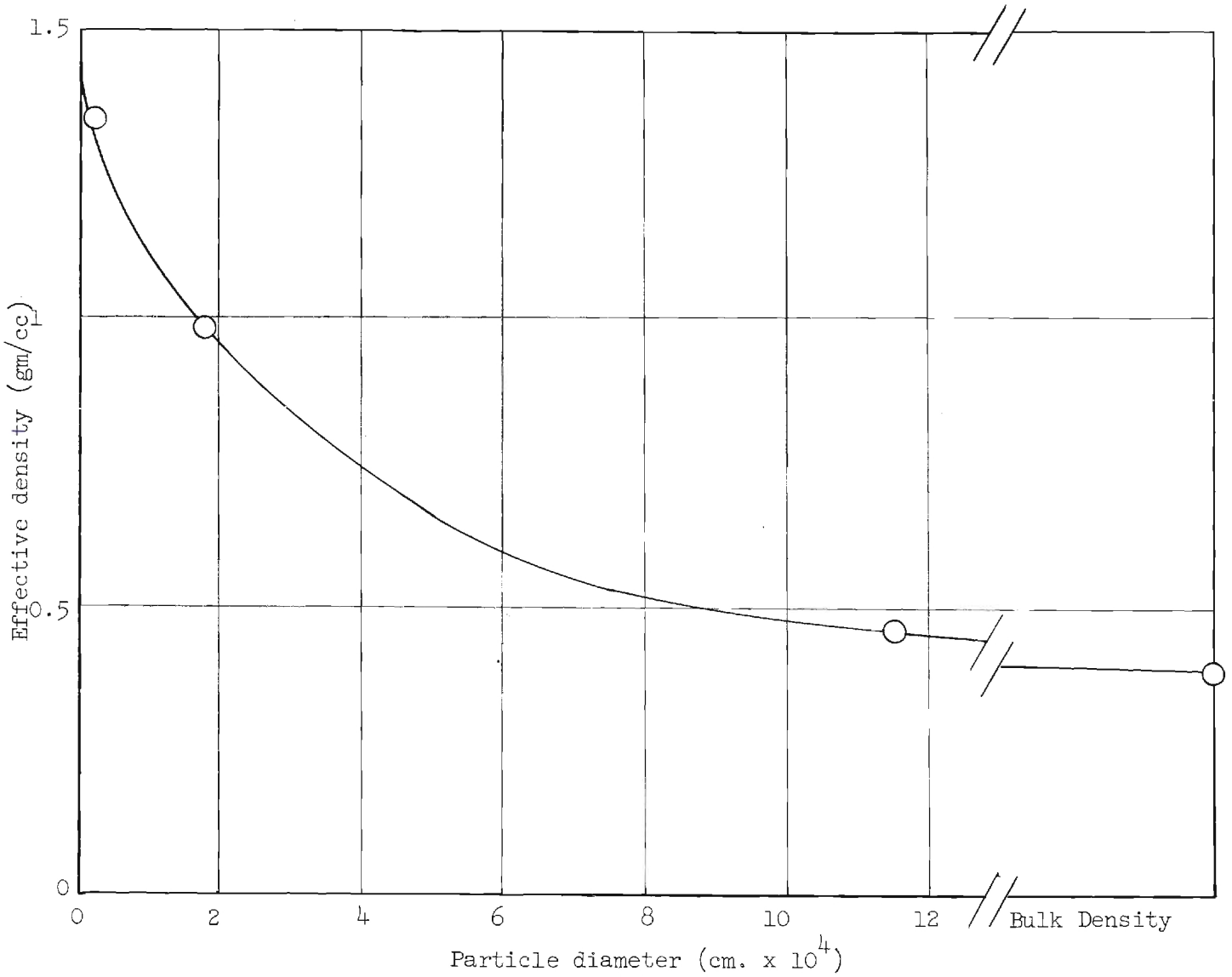

Figure 13. Effective Density versus Particle Diameter for Wood Charcoal.

APPENDIX B

TABULATIONS AND GRAPHIC PRESENTATIONS OF EXPERIMENTAL DATA

Table 3. Experimental Data* for Gas Carbon Particles

Settling Velocity (cm/sec)	Rising Velocity (cm/sec)	Radius (microns)	Photophoretic Force (dynes x 10^6)
	Pressure = 4.4 mm. Hg		
0.741	0.452	21.2	4.22
1.06	0.555	20.6	4.39
0.771	0.582	16.0	2.54
0.411	0.785	10.5	1.36
0.457	0.456	11.9	1.23
0.456	0.304	12.1	1.03
0.588	0.430	13.4	1.45
0.380	0.418	10.1	0.792
0.760	0.925	17.1	4.24
0.644	0.377	14.4	1.60
	Pressure = 10.0 mm. Hg		
0.516	0.188	20.3	3.02
0.550	0.158	21.2	3.21
0.541	0.300	20.7	3.79
0.590	0.279	22.0	4.22
0.645	0.222	23.1	4.41
0.387	0.149	17.3	1.93
0.349	0.214	16.2	1.89
0.560	0.224	21.4	3.80
0.525	0.321	20.6	3.88
0.261	0.223	13.9	1.42
0.345	0.240	16.2	2.00
0.420	0.358	18.3	3.18
0.430	0.262	18.4	2.78
0.430	0.230	18.6	2.70
0.306	0.178	15.3	1.55
	Pressure = 14.3 mm. Hg		
0.451	0.243	19.7	3.23
0.338	0.266	16.9	2.42
0.543	0.190	21.9	3.75
0.316	0.318	16.1	2.41
0.268	0.152	14.7	1.38
0.405	0.197	18.6	2.61
0.254	0.304	14.4	1.88
0.324	0.197	16.4	1.95
0.338	0.213	16.8	2.15
0.316	0.304	16.3	2.40

(Continued)

Table 3. (Continued)

Settling Velocity (cm/sec)	Rising Velocity (cm/sec)	Radius (microns)	Photophoretic Force (dynes x 10^6)
	Pressure = 20.1 mm. Hg		
0.296	0.203	16.2	1.99
0.384	0.227	18.6	2.83
0.473	0.144	20.9	3.12
0.258	0.152	15.0	1.48
0.352	0.258	17.8	2.73
0.254	0.213	14.9	1.72
0.273	0.227	15.5	1.92
0.203	0.202	13.2	1.31
0.211	0.182	13.4	1.27
0.741	0.304	26.5	7.02
0.423	0.221	19.7	3.16
0.278	0.137	15.7	1.56
	Pressure = 25.8 mm. Hg		
0.463	0.153	20.9	3.23
0.184	0.073	12.8	0.782
0.286	0.167	16.2	1.84
0.249	0.109	15.0	1.32
0.304	0.121	16.8	1.77
0.374	0.146	18.7	2.42
0.356	0.113	18.2	2.11
0.168	0.121	12.2	0.872

*Light Intensity = 0.185 watts/cm^2

Table 4. Experimental Data* for Gas Carbon Particles

Settling Velocity (cm/sec)	Rising Velocity (cm/sec)	Radius (microns)	Photophoretic Force (dynes x 10^6)
	Pressure = 8.3 mm. Hg		
0.532	0.410	20.0	3.98
0.418	0.337	17.4	2.67
0.769	0.789	24.8	8.87
0.659	0.582	22.8	6.32
0.472	0.501	18.8	3.94
1.065	0.797	30.0	1.31
0.672	0.592	23.2	6.66
0.633	0.763	22.5	7.28
0.600	0.919	21.9	7.79
0.567	0.600	21.2	5.60
0.633	0.789	22.2	7.13
0.426	0.589	17.6	3.78
0.461	0.589	18.5	4.17
	Pressure = 15.3 mm. Hg		
0.252	0.214	14.0	1.47
0.644	0.528	24.1	7.17
0.558	0.543	22.3	6.24
0.341	0.435	17.1	3.29
0.483	0.439	20.7	4.79
0.279	0.342	15.3	2.31
0.380	0.430	18.2	3.68
0.535	0.488	21.8	5.60
0.555	0.403	22.2	5.27
0.500	0.337	21.0	4.29
0.292	0.228	15.6	2.14
0.303	0.298	15.9	2.28
0.475	0.380	20.4	4.31
	Pressure = 25.6 mm. Hg		
0.281	0.218	16.1	2.06
0.218	0.202	12.1	1.13
0.216	0.091	12.0	0.744
0.433	0.372	18.1	3.10
0.190	0.216	11.2	1.02
0.417	0.270	17.8	2.83
0.525	0.234	20.3	3.51
0.184	0.373	11.0	1.49
0.450	0.302	18.6	3.29
0.389	0.350	17.1	2.60

(Continued)

Table 4. (Continued)

Settling Velocity (cm/sec)	Rising Velocity (cm/sec)	Radius (microns)	Photophoretic Force (dynes x 10^6)
	Pressure = 35.4 mm. Hg		
0.336	0.288	18.0	2.75
0.081	0.169	8.4	0.551
0.166	0.249	12.4	1.40
0.469	0.255	21.4	3.80
0.514	0.349	22.5	4.09
0.333	0.231	17.9	2.70
0.239	0.161	15.0	1.58
0.174	0.225	12.7	1.36
	Pressure = 46.0 mm. Hg		
0.383	0.200	19.5	3.05
0.346	0.165	18.5	2.52
0.245	0.220	15.4	1.97
0.208	0.234	14.2	1.74
0.378	0.172	19.3	2.84
0.303	0.214	17.2	2.43
0.317	0.186	17.6	2.40
0.210	0.207	14.2	1.63
0.292	0.214	16.9	2.34

*Light Intensity = 0.25 watts/cm^2

Table 5. Experimental Data* for Wood Charcoal Particles

Settling Velocity (cm/sec)	Rising Velocity (cm/sec)	Radius (microns)	Photophoretic Force (dynes x 10^6)
	Pressure = 4.7 mm. Hg		
0.728	0.605	6.61	0.751
0.778	0.605	7.26	0.960
0.675	0.307	6.56	0.559
0.700	0.285	6.84	0.608
0.936	0.679	8.09	1.28
0.748	0.471	6.76	0.701
0.724	0.364	6.85	0.663
0.734	0.437	7.02	0.763
1.57	0.550	11.9	3.10
1.66	0.564	12.8	3.77
1.10	1.02	9.69	2.50
	Pressure = 9.7 mm. Hg		
1.18	0.486	12.5	3.80
0.840	0.263	10.2	1.86
0.460	0.223	6.92	0.671
1.00	0.573	11.5	3.30
0.645	0.384	8.74	1.47
0.555	0.338	7.94	1.11
1.09	0.343	12.1	3.16
	Pressure = 15.6 mm. Hg		
0.538	0.419	3.96	0.187
0.446	0.202	4.91	0.365
0.337	0.320	4.07	0.321
0.199	0.168	2.22	0.0657
0.506	0.138	5.29	0.365
0.594	0.193	6.90	0.688
0.286	0.220	3.17	0.157
0.270	0.110	3.06	0.100
0.308	0.219	3.36	0.180
0.730	0.408	7.90	1.32
0.212	0.107	2.31	0.0551
0.452	0.212	4.98	0.387
0.374	0.237	4.38	0.311

(Continued)

Table 5. (Continued)

Settling Velocity (cm/sec)	Rising Velocity (cm/sec)	Radius (microns)	Photophoretic Force (dynes x 10^6)
	Pressure = 21.3 mm. Hg		
0.118	0.0808	2.44	0.0603
0.401	0.205	7.80	0.982
0.366	0.164	7.39	0.795
0.368	0.151	7.45	0.788
0.589	0.311	9.70	1.91
0.273	0.152	6.18	0.507
0.381	0.174	7.57	1.86
0.270	0.182	6.17	0.550
0.376	0.222	7.52	0.937
0.479	0.222	8.61	1.27
0.521	0.300	9.04	1.60

*Light Intensity = 0.25 watts/cm^2

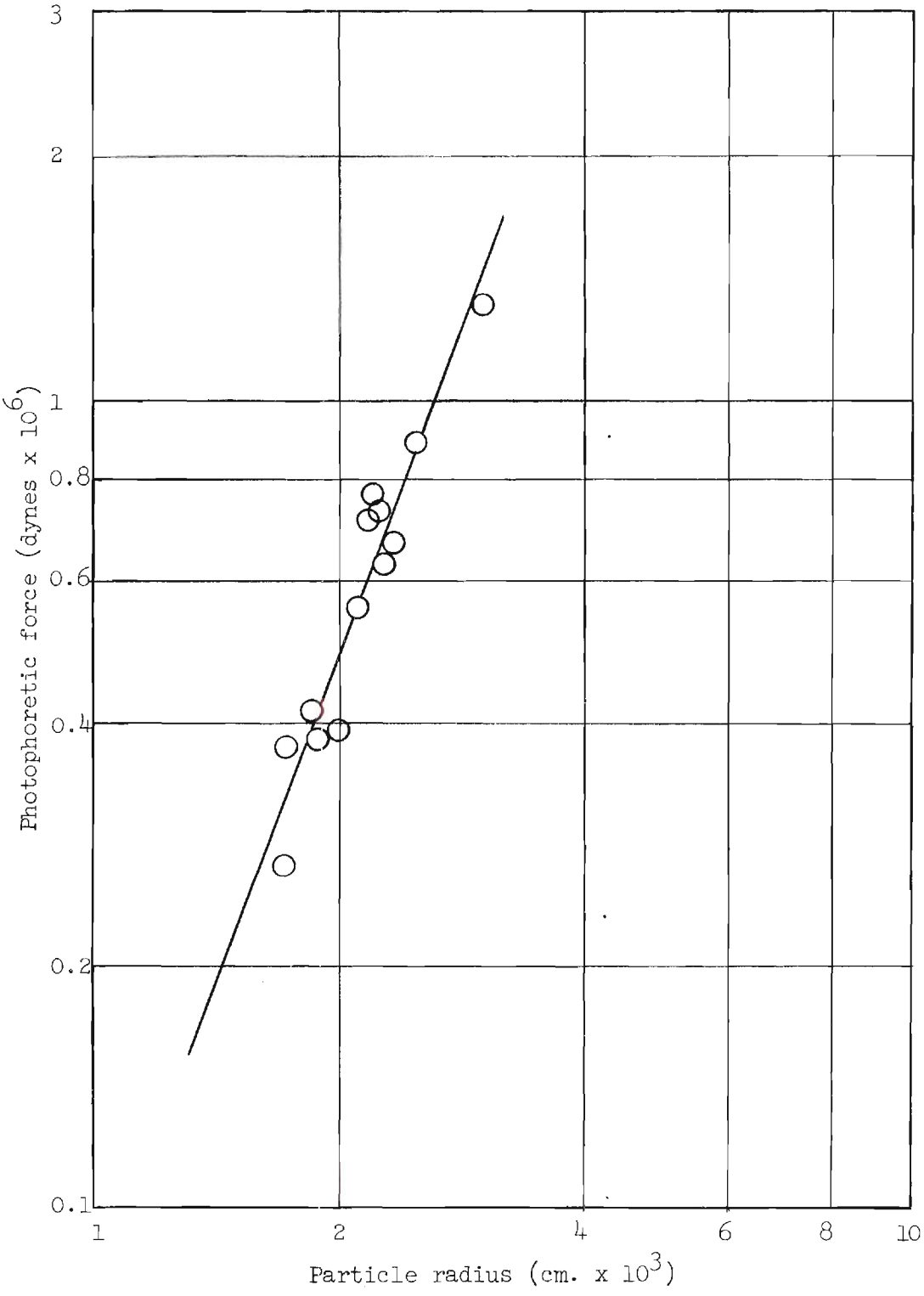

Figure 14. Photophoretic Force versus Particle Radius for Gas Carbon at 8.3 mm. Hg.

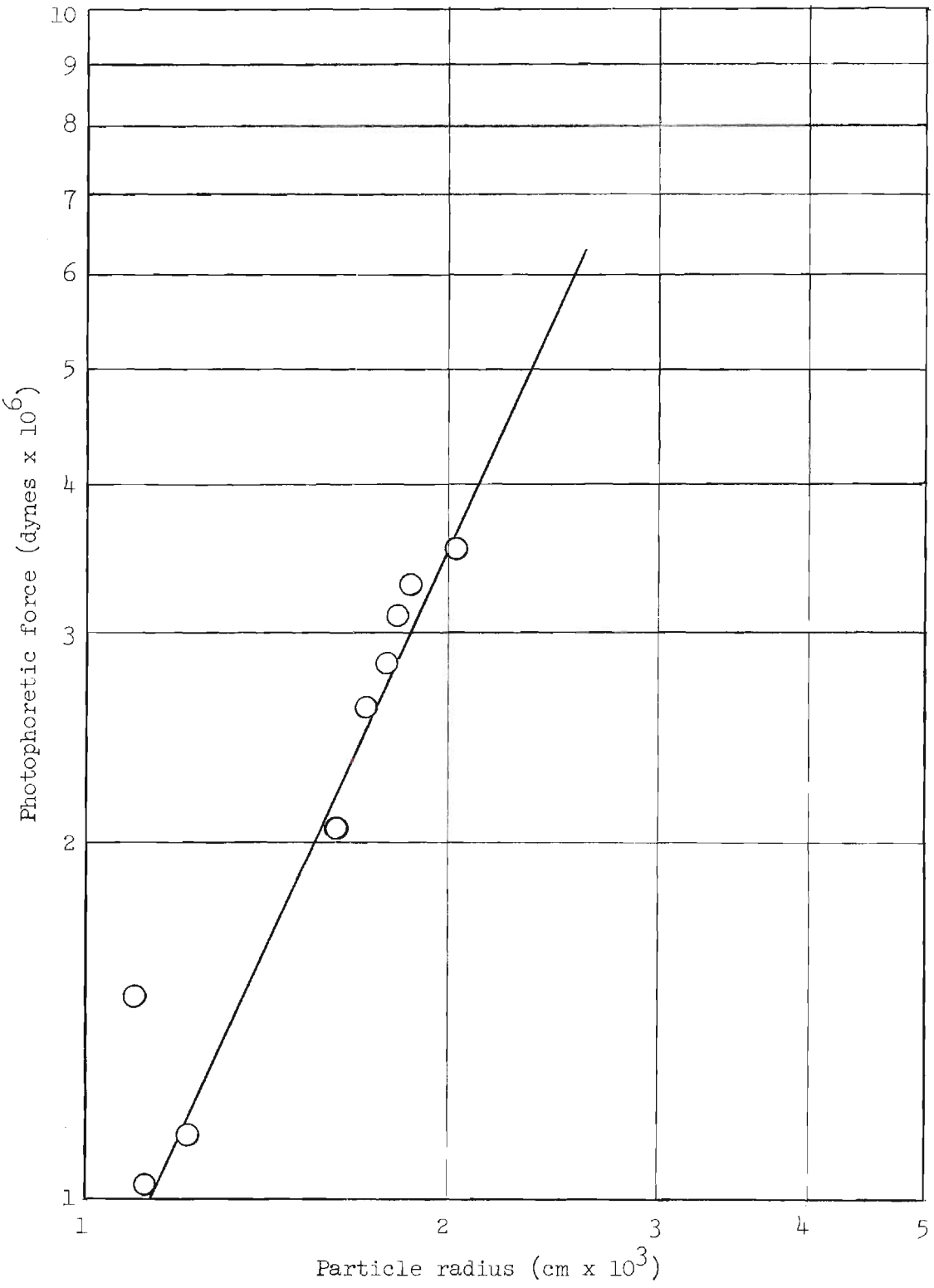

Figure 15. Photophoretic Force versus Particle Radius for Gas Carbon at 25.6 mm. Hg.

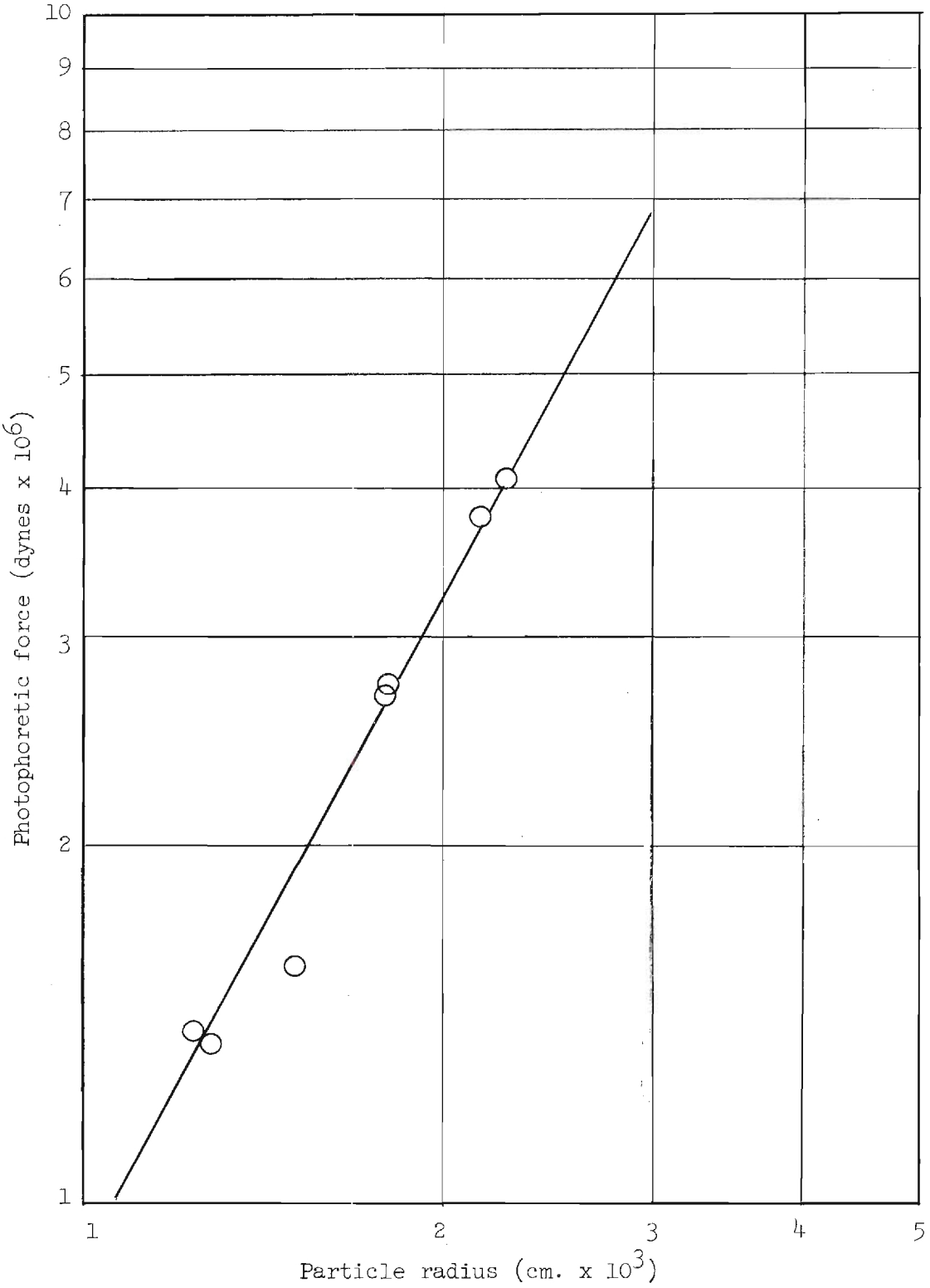

Figure 16. Photophoretic Force versus Particle Radius for Gas Carbon at 35.4 mm. Hg.

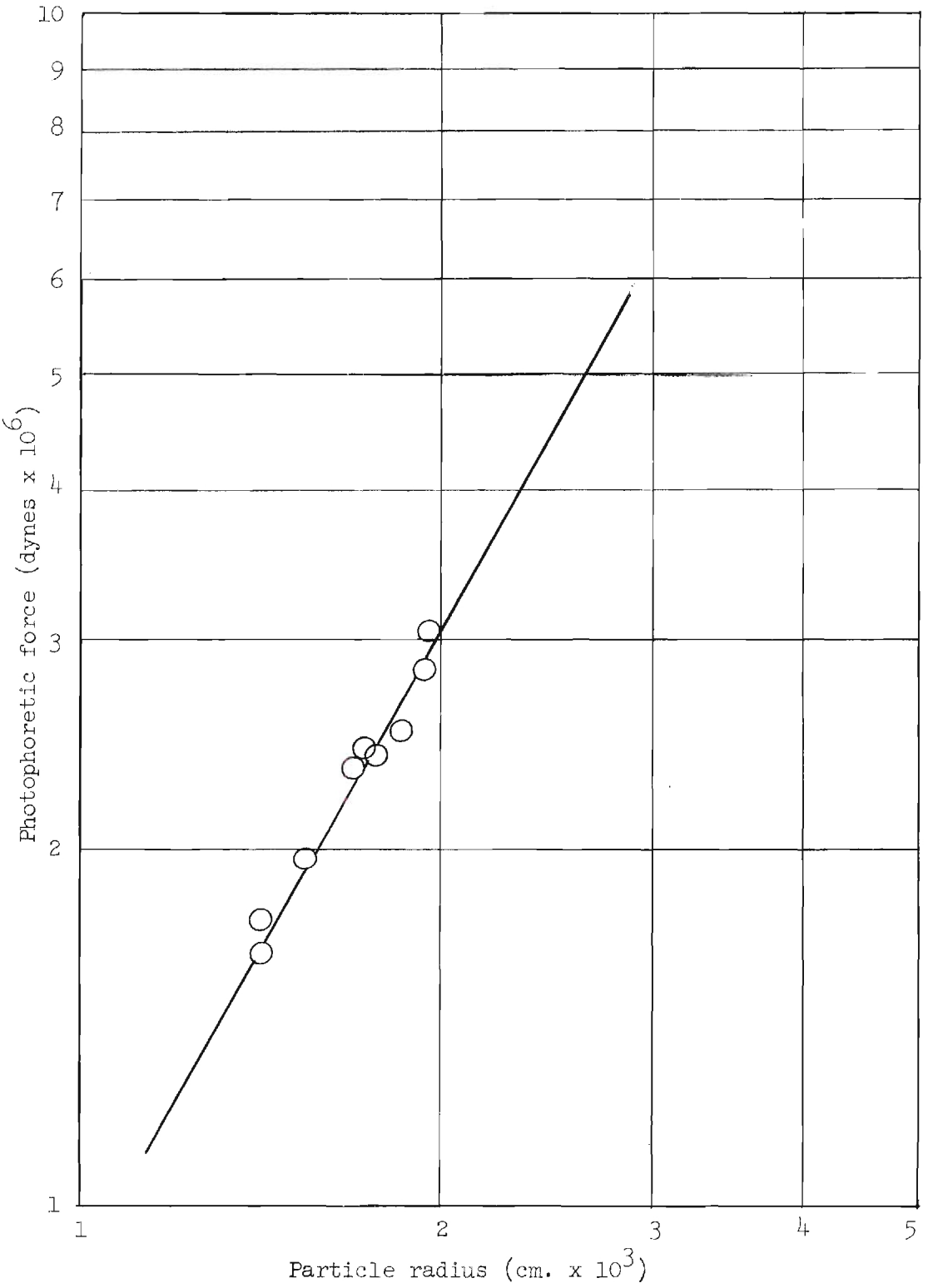

Figure 17. Photophoretic Force versus Particle Radius for Gas Carbon at 46.0 mm. Hg.

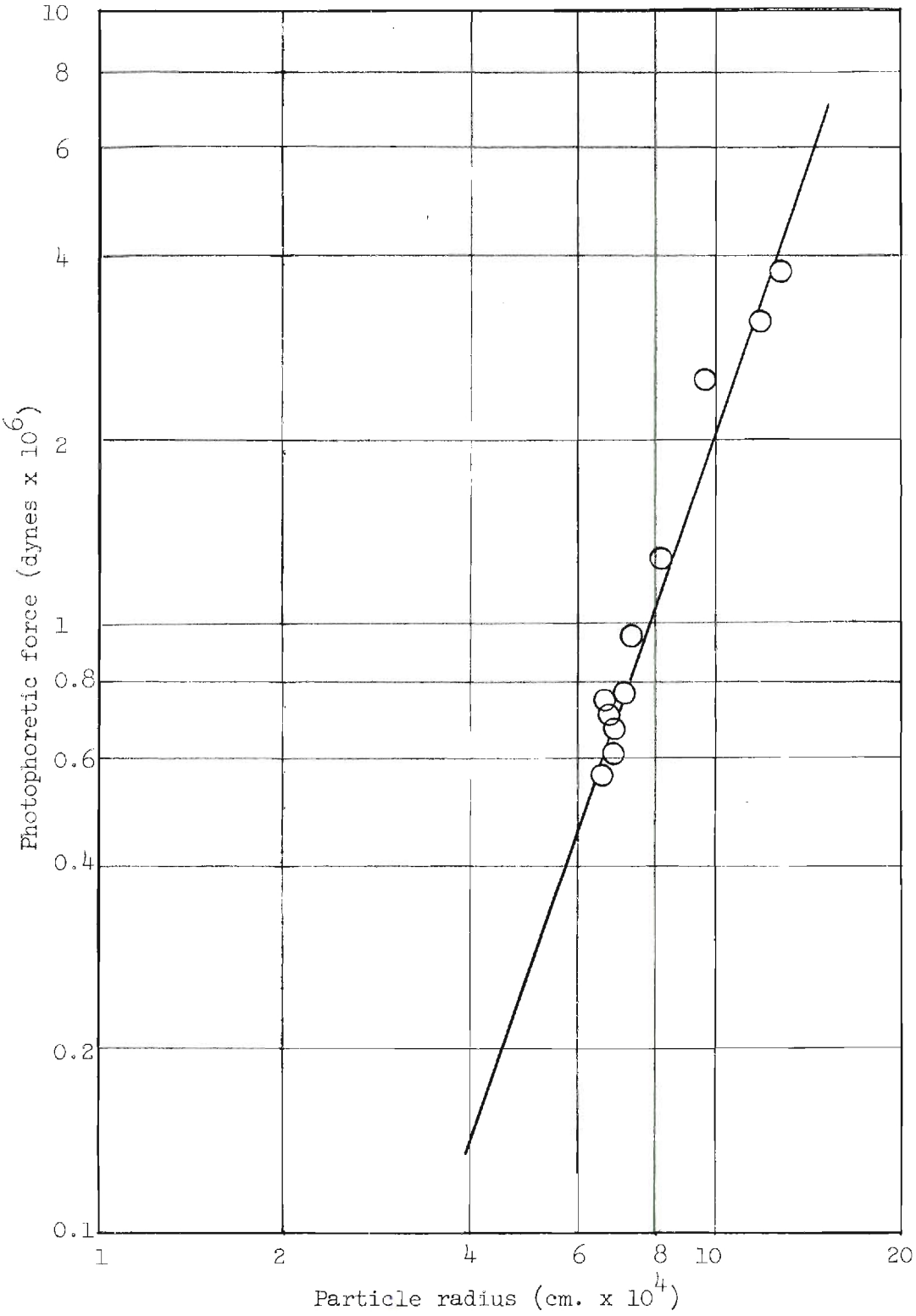

Figure 18. Photophoretic Force versus Particle Radius for Wood Charcoal at 4.7 mm. Hg.

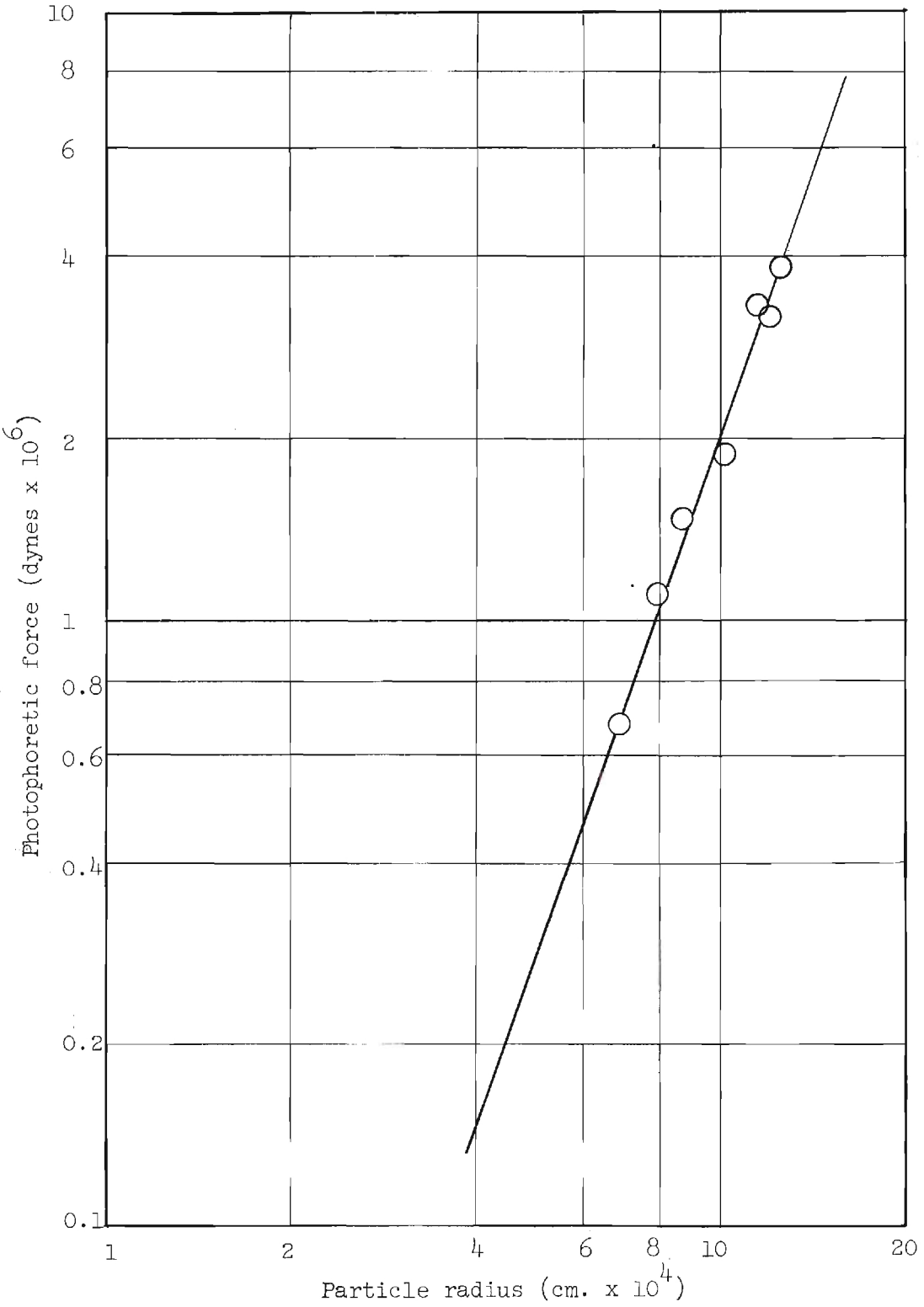

Figure 19. Photophoretic Force versus Particle Radius for Wood Charcoal at 9.7 mm. Hg.

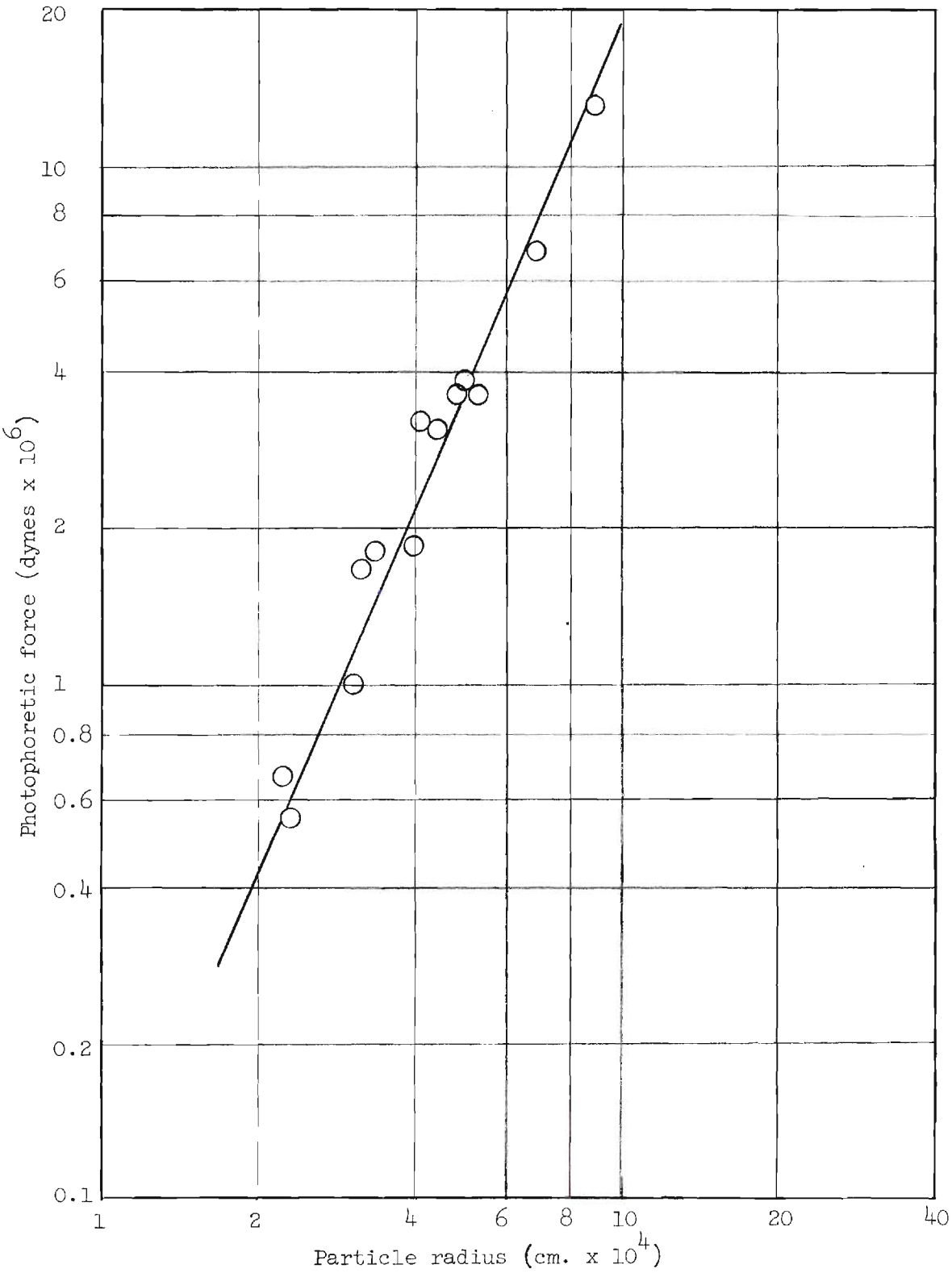

Figure 20. Photophoretic Force versus Particle Radius for Wood Charcoal at 15.6 mm. Hg.

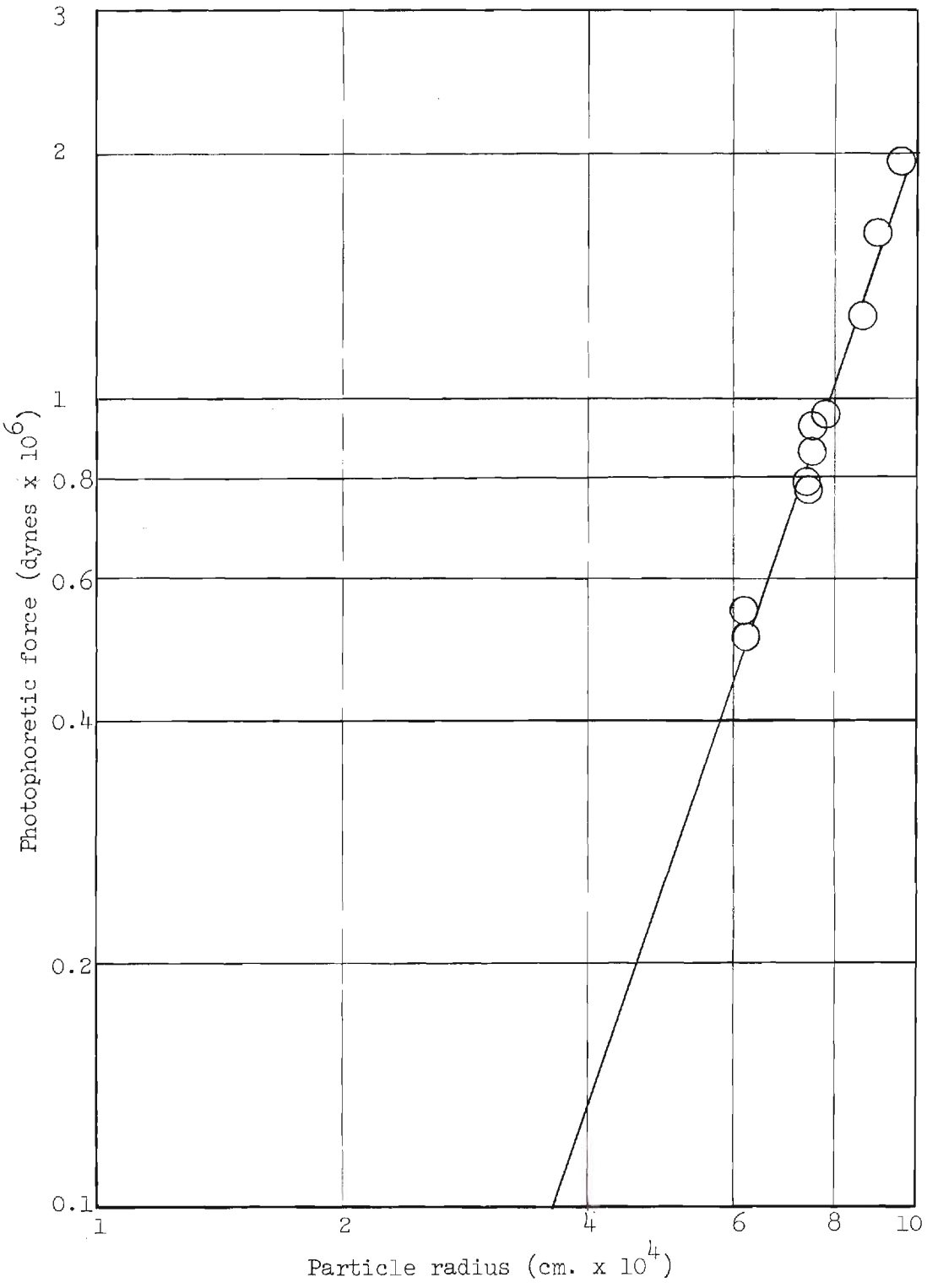

Figure 21. Photophoretic Force versus Particle Radius for Wood Charcoal at 21.3 mm. Hg.

BIBLIOGRAPHY

1. F. Ehrenhaft, "Über die Messung von Elektrizitatsmengen, die kleiner zu sein scheinen als die Ladung des einvertigen Wasserstoffions oder Elektron and von dessen Vulfachen abweichen," Wiener Berichte 119, IIa, 815-866 (1910).

2. F. Ehrenhaft, "Die Photophorese," Annalen der Physik 56, 81-132 (1918).

3. O. Preining, "The Phenomena of Photophoresis," Staub 39, 45-64 (1955).

4. G. Hettner, "Zur Theorie der Photophorese," Zeitschrift für Physik 37, 179-192 (1926).

5. A. Rubinowitz, "Radiometerkräfte und Ehrenhaftsehe Photophorese," Annalen der Physik 62, 691-715 (1920).

6. H. Rohatschek, "Theory of Photophoresis, Results and Problems," Staub 42, 607-643 (1955).

7. J. Mattauch, "Neue Versuch zur Photophorese," Physikalische Zeitschrift 23, 44-448 (1922).

8. C. M. Swenne, Thyratrons, New York, Macmillan (1960).

9. I. Mattauch, "Eine experimentelle Ermittlung des Widerstandsgesetzes kleiner Kugeln in Gasen," Zeitschrift fur Physik 32, 439-472 (1925).

10. E. Cunningham, "On the Velocity of Steady Fall of Spherical Particles through Fluid Medium," Proceedings of the Royal Society 83A, 357-365 (1910).

11. R. A. Millikan, "Coefficients of Slip in Gases and the Law of Reflection from the Surfaces of Solids and Liquids," Physical Review 21, 217-238 (1923).

12. C. N. Davies, "Definitive Equations for the Fluid Resistance of Spheres," Proceedings of the Physical Society 57, 259-270 (1945).

13. M. Knudsen and S. Weber, "Luftwiderstand gegen die langsame Bewegung in Gasen," Zeitschrift für Physik 32, 981-994 (1911).

14. P. Tauzin, "Negative Photophoresis in Relation to a Recent Radiometer Experiment," Academie des Sciences, Paris 234, 2265-2267 (1952).

15. P. Tauzin, "La Phophorese," Genie Chemique 74, 33-7 (1955).

16. J. Thibaud, M. Maitrot and J. Berthier, "Properties of Thin Films and Radiometric Interpretation of Longitudinal Photophoresis," Academie des Sciences, Paris 231, 691-3 (1950.

17. K. H. Baldenhol, "On the Properties of Intensely Illuminated Suspended Particles in Magnetic and Electric Fields," Annalen des Physik (Leipzig) 14, 17-32 (1954).

18. P. S. Epstein, "Zur Theorie der Radiometers," Zeitschrift für Physik 54, 537-563 (1929).

19. S. Weber, "D. Kgl. Danske Vidensk. Sebsk.," Math-fys Medd XXI (1944).

20. A. Cotton, "Explanation of the Phenomena of Photophoresis," Academie des Sciences, Paris 225, 969-972 (1947).

21. F. Ehrenhaft, "On Photophoresis, the True Magnetic Charge, and the Helical Motion of Matter in Various Fields I," Acta Physica Austriaca 4, 461-88 (1951).

22. F. Ehrenhaft, "Photophoresis and its Interpretation by Electric and Magnetic Ions," Journal of the Franklin Institute 233, 235-254 (1942).

23. N. A. Fuks, (Academy of Sciences of the U.S.S.R. Institute of Scientific Information), The Mechanics of Aerosols, CWS Special Publication 4-12, U. S. Army Chemical Welfare Laboratories, Army Chemical Center, Maryland (1955) p. 34.

24. R. G. Deissler and C. S. Eian, "An Investigation of Effective Thermal Conductivities of Powders," National Advisory Committee on Aeronautics, RM E52C05 (1952).

25. R. G. Deissler and J. S. Boegli, "An Investigation of Effective Thermal Conductivities of Powders in Various Gases," Transactions of the American Society of Mechanical Engineers 80, 1417-23 (1958).

26. W. Schotte, "Thermal Conductivity of Packed Beds," Journal of the American Institute of Chemical Engineers 6, No. 1, 63-67 (1960).